JOURNAL OF GEOPHYSICAL RESEARCH, VOL. 113, B10304, doi:10.1029/2007JB005497, 2008

Click Here for Full Article

Lithospheric structure of the Bohemian Massif and adjacent Variscan belt in central Europe based on profile S01 from the SUDETES 2003 experiment

Marek Grad,[1] Aleksander Guterch,[2] Stanisław Mazur,[3,4] G. Randy Keller,[5] Aleš Špičák,[6] Pavla Hrubcová,[6] and Wolfram H. Geissler[7,8]

Received 13 November 2007; revised 20 June 2008; accepted 8 July 2008; published 4 October 2008.

[1] The SUDETES 2003 seismic experiment investigated the lithospheric structure of the eastern part of the Variscan belt of central Europe. The key profile of this experiment (S01) was 630 km long and extended southwestward from the margin of the East European craton, across the Trans-European suture zone (TESZ) and Sudetes, and across the Bohemian Massif that contains the active Eger (Ohře) rift, which is an element of the European Cenozoic rift system. Good quality first arrivals and later phases of refracted/reflected *P* and *S* waves were interpreted using 2-D ray-tracing techniques. The derived seismic model shows large variations in the internal structure of the crust, while the depth to the Moho varies in the relatively narrow depth interval of 28–35 km. Except for the Polish basin on the northeast end of the profile, the sedimentary cover is thin. The crystalline upper and middle crust with velocities of 5.9–6.4 km s^{-1} is about 20 km thick, and the 7–10 km thick lower crust can be divided into three regions based on *P* wave velocities: a low-velocity region (6.5–6.6 km s^{-1} beneath Eger rift and Sudetes) that is bounded on the southwest and northeast by regions of significantly higher velocity (6.8–7.1 km s^{-1} beneath the Saxothuringian and Moldanubian in the southwest and Fore-Sudetic Monocline and Polish Basin in the northeast). High-velocity bodies ($Vp > 6.5$ km s^{-1}) were delineated in the upper crust of the Eger rift region. The seismic structure along the S01 profile images a Variscan orogenic wedge resting on the down warped margin of the plate margin containing the TESZ. This situation implies the northerly directed subduction of the Rheic Ocean that existed between the southern margin of the Old Red Continent and the Armorican terranes presently accreted into the Variscan belt. Closure of this ocean produced the Rheic suture between low-velocity crust of the Variscan orogenic wedge and higher-velocity crust of the TESZ.

Citation: Grad, M., A. Guterch, S. Mazur, G. R. Keller, A. Špičák, P. Hrubcová, and W. H. Geissler (2008), Lithospheric structure of the Bohemian Massif and adjacent Variscan belt in central Europe based on profile S01 from the SUDETES 2003 experiment, *J. Geophys. Res.*, *113*, B10304, doi:10.1029/2007JB005497.

1. Introduction

[2] Spanning 7 years (1997–2003), four large seismic experiments (POLONAISE'97, CELEBRATION 2000, ALP 2002, and SUDETES 2003) were conducted in central Europe between the Baltic and Adriatic seas (Figures 1 and 2). This unprecedented network of seismic refraction experiments involved a massive international collaboration involving geophysicists from Europe and North America (about 40 institutions from 17 countries). A primary scientific goal of these experiments was to investigate the lithospheric structure of the southwestern margin of the East European craton (EEC) and its relation to accreted younger terranes to the southwest. The target of the POLONAISE'97 experiment was the Trans-European suture zone (TESZ) and the transition from the EEC to the Paleozoic platform [*Guterch et al.*, 1998, 1999]. The transition from the EEC through the Carpathian Mountains to the Pannonian basin and to the Bohemian Massif was a major target of the CELEBRATION 2000 experiment [*Guterch et al.*, 2000, 2001, 2003b], and the Eastern Alps and the transition to the Bohemian Massif were major targets of the ALP 2002 experiment [*Brückl et al.*, 2003, 2007]. The SUDETES

[1]Institute of Geophysics, University of Warsaw, Warsaw, Poland.
[2]Institute of Geophysics, Polish Academy of Sciences, Warsaw, Poland.
[3]Institute of Geological Sciences, University of Wrocław, Wrocław, Poland.
[4]Now at GETECH, Leeds, UK.
[5]School of Geology and Geophysics, University of Oklahoma, Norman, Oklahoma, USA.
[6]Geophysical Institute, Academy of Science of the Czech Republic, Prague, Czech Republic.
[7]GeoForschungsZentrum-Potsdam, Potsdam, Germany.
[8]Now at Alfred Wegener Institute for Polar and Marine Research, Bremerhaven, Germany.

0148-0227/08/2007JB005497$09.00

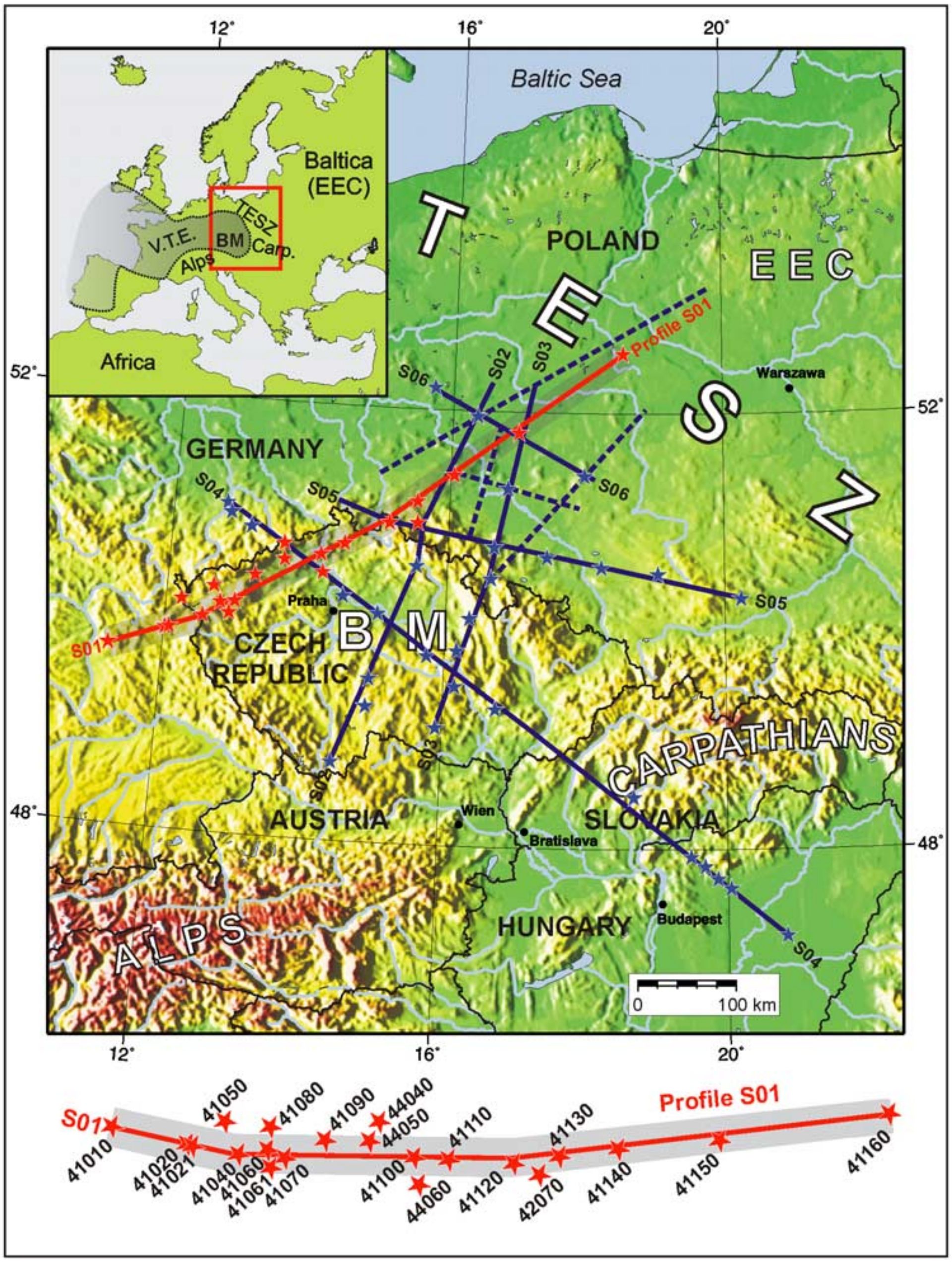

Figure 1. Location of the S01 profile together with other SUDETES 2003 profiles S02–S06. Red stars refer to the location of 21 shotpoints along the S01 profile (red line) that were used in this paper. Table 1 provides detailed information about these shotpoints. Blue stars refer to shotpoints on other profiles marked as blue solid lines; dashed lines refer to additional recording profiles. Red rectangle in the insert shows the study area; European Variscides marked in gray; BM, Bohemian Massif; Carp., Carpathians; EEC, East European craton; TESZ, Trans-European suture zone; V.T.E., Variscan terranes of Europe. The S01 profile with shot numbers is shown below the map.

2003 experiment was designed to link with these previous experiments and focus on Variscan structures of the Bohemian Massif and its surroundings [*Grad et al.*, 2003b; *Guterch et al.*, 2003a]. The tectonic evolution of this region is of global importance to studies of terrane tectonics, rifting, orogenesis and continental evolution.

[3] It should be noted that all four of these experiments were 3-D in nature in that, to the extent possible, all shots were designed to be recorded by all in-line and off-line recorders. Thus, the ultimate goal of this effort is a consistent 3-D interpretation of all existing data in the vast area covered by these experiments. However, to date, 3-D analyses have been completed only for selected regions: the TESZ and EEC in central Poland [*Środa et al.*, 2002; *Czuba et al.*, 2002], the Eastern Alps [*Behm et al.*, 2006, 2007], the northern Bohemian Massif [*Majdański et al.*, 2007], southeast Poland in the transition from the EEC to the Carpathians [*Malinowski et al.*, 2008], and a local area in the northeastern Pannonian basin [*Hajnal et al.*, 2004].

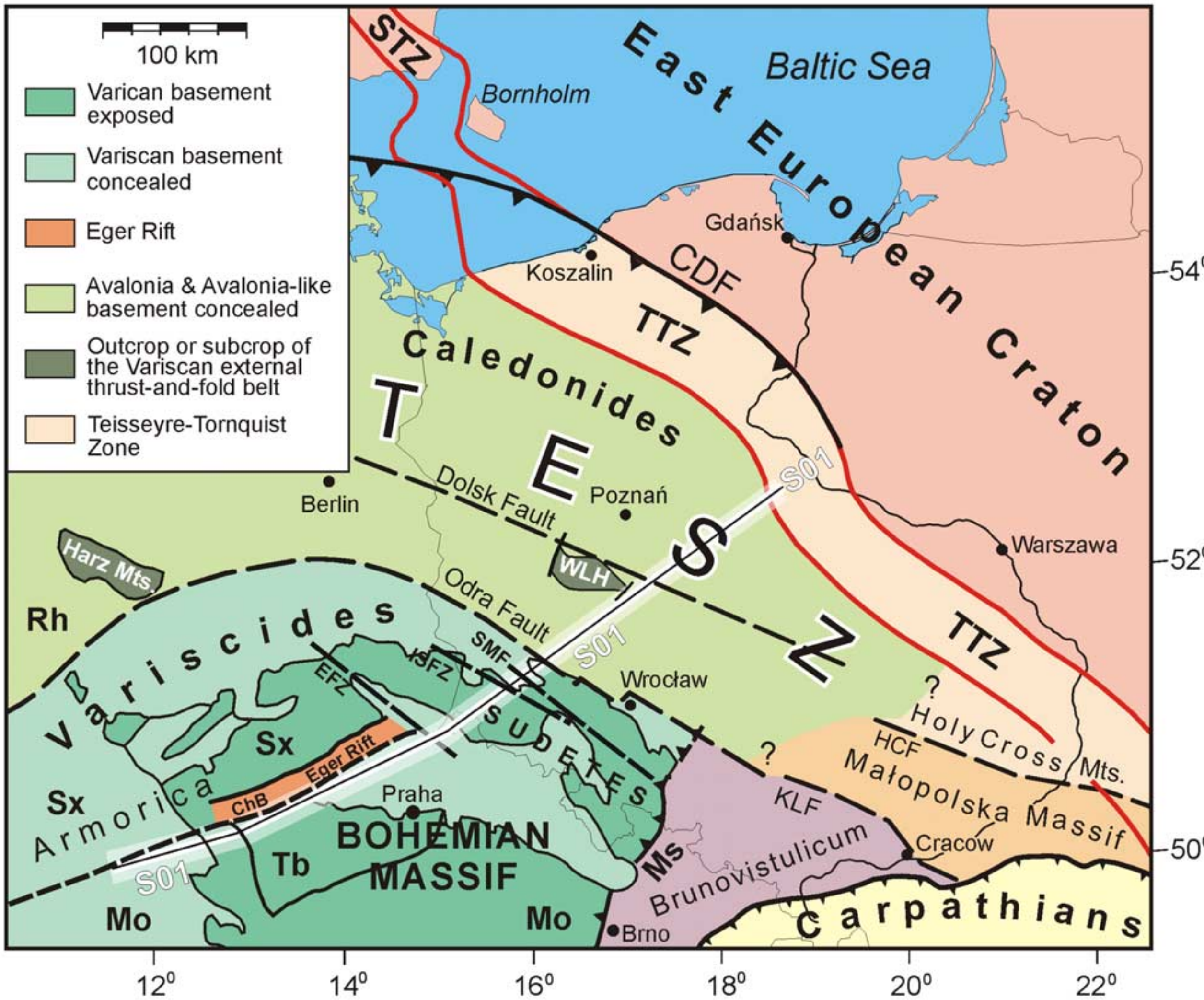

Figure 2. Main basement units of the TESZ and eastern Variscan belt [*Mazur and Jarosiński*, 2006] in the area crossed by the S01 profile, which is shown as a highlighted thin black line. CDF, Caledonian deformation front; ChB, Cheb basin; EFZ, Elbe fault zone; HCF, Holy Cross fault; ISFZ, Intra-Sudetic fault zone; KLF, Kraków-Lubliniec fault; Mo, Moldanubian zone; Ms, Moravosilesian zone; Rh, Rhenohercynian zone; SMF, Sudetic Marginal fault; STZ, Sorgenfrei-Tornquist zone; Sx, Saxothuringian zone; Tb, Teplá-Barrandian zone; TESZ, Trans-European suture zone; TTZ, Teisseyre-Tornquist zone; WLH, Wolsztyn-Leszno High.

[4] The 630 km long S01 profile (Figure 1) is the subject of this paper, and our analysis combined with recent results from other profiles in the area provides comprehensive seismic coverage of the Bohemian Massif and the transition across the Variscan belt to the TESZ [*Grad et al.*, 2003a, 2006; *Hrubcová et al.*, 2005, 2008; *Wilde-Piórko et al.*, 2005; *Środa et al.*, 2006]. The first results published from the evaluation of the shorter SUDETES 2003 profiles [*Majdański et al.*, 2006; *Růžek et al.*, 2007] and 3-D structure [*Majdański et al.*, 2007] provide a context for our analysis. In this paper, we summarize available geophysical information and data with the emphasize on reconciling possible geophysical models with geological concepts concerning crustal structure across the transition from the Variscan belt to its northern foreland. Eventually, we propose a conceptual geodynamic model providing a scenario for accretion of the Variscan terranes to the SW margin of the TESZ.

2. Regional Geological and Geophysical Setting

[5] The S01 profile traverses two important crustal domains extending between the edge of the EEC and the interior of the Variscan belt. The northeastern domain that forms the basement of the Paleozoic platform of southwest Poland corresponds to the TESZ that represents a broad and complex zone of early Paleozoic terrane accretion to the southwest margin of Baltica [*Pharaoh*, 1999]. Alternatively, the area of the TESZ has been defined as a passive Baltica margin buried beneath a thick cover of upper Paleozoic and Mesozoic sediments [*Berthelsen*, 1998]. The crust of the TESZ shows peculiar characteristics distinct from the adjacent areas. It is relatively thin (30–32 km) with a three-layer

seismic velocity structure [e.g., *Guterch et al.*, 1986, 1992; *Grad et al.*, 2002a; *Malinowski et al.*, 2005]. The upper crust, up to 15–18 km thick, reveals low *P* wave velocities below 6 km s^{-1} and is interpreted to consist of a low-grade metamorphosed volcano-sedimentary succession [*Grad et al.*, 2002a] or, alternatively, highly sheared granitic/gneissic basement with a NW–SE oriented anisotropy following the trend of the TESZ [*Jarosiński and Dąbrowski*, 2006]. The lower crust, only 8–10 km thick, is a high-velocity layer (7.1 km s^{-1}) with ringing reflectivity. The origin of the lower crust in the TESZ domain can be explained by (1) southwestward underthrusting of an attenuated EEC margin beneath sediments of the Avalonian accretionary prism [*Grad et al.*, 2002a]; (2) its being the lower crust of two Baltica-derived early Paleozoic terranes (Kuiavia and Pomerania) accreted in the TESZ [*Dadlez et al.*, 2005]; or (3) its being part of the rifted EEC passive margin that developed in the early Paleozoic and is onlapped by an autochthonous sedimentary succession [*Dadlez*, 1978, 2000; *Berthelsen*, 1998; *Keller and Hatcher*, 1999; *Grad et al.*, 2003a]. Regardless of the favored interpretation, it is in generally agreed that the area of the TESZ from Early Devonian times belonged to the southern margin of the Old Red Continent formed because of the early Paleozoic amalgamation of Laurentia, Baltica, and Avalonia [e.g., *Tait et al.*, 2000]. The sedimentary cover of the TESZ comprises the NW–SE elongated depocenters of the Permo-Mesozoic Polish basin with thickness of sedimentary fill in the range of 4–8 km underlain to the southwest by the Carboniferous strata of a Variscan foreland basin. Consequently, the deep early Paleozoic basement of the TESZ below the Polish basin is not penetrated by wells and its origin remains a matter of speculation. A model of possible basement structure of the TESZ along the northeast section of S01 line can be presumed by extrapolating subsurface data from the area of the North German-Pomeranian Caledonides (Figure 2) that show intensely deformed early Paleozoic sediments unconformably overlain by the late Paleozoic platform succession [*Dadlez*, 1978, 2000]. However, the southeastward extent of Caledonian deformation in Poland is unknown.

[6] The southwest domain traversed by the S01 profile corresponds to the European Variscan belt that is traditionally divided in the area of the Bohemian Massif into the Saxothuringian, Moldanubian and Teplá-Barrandian tectonostratigraphic zones [*Kossmat*, 1927; *Malkovský*, 1979]. The Saxothuringian zone comprises several occurrences of high-grade rocks interpreted as nappes and/or basement domes accompanied by a low-grade at least partly autochthonous volcano-sedimentary succession of Ordovician through Early Carboniferous age (see *Franke* [2000] for overview). The southeast contact of the Saxothuringian zone against the adjacent Moldanubian and Teplá-Barrandian zones is supposed to constitute a tectonic suture formed because of the Late Devonian/Early Carboniferous closure of the Saxothuringian Ocean, which was branch of the Rheic Ocean [e.g., *Franke et al.*, 1995; *Franke*, 2000; *Krawczyk et al.*, 2000]. This suture is identified by occurrences of (U)HP granulites and eclogites as well as bodies of ultramafic rocks and believed to represent a root zone for nappes thrust over the Saxothuringian domain [e.g., *Franke et al.*, 1995]. The Teplá-Barrandian zone (Figure 2) consists of nearly 10 km thick succession of mostly low-grade to unmetamorphosed upper Proterozoic sediments resting on the unknown basement. The Precambrian rocks are unconformably overlain by a Cambrian to Devonian succession of unmetamorphosed sediments and volcanics [e.g., *Chaloupský et al.*, 1995]. The Moldanubian zone represents the southern part of the Bohemian Massif comprising mostly medium- to high-grade gneisses and migmatites of supracrustal origin with late HT metamorphic overprint accompanied by voluminous intrusions of Carboniferous granites. The zone corresponds to the root of the Variscan orogen and continues toward the southwest into the Schwarzwald, Vosges, and Massif Central [e.g., *Matte et al.*, 1990; *Franke*, 2000]. The classical tectonostratigraphic zones of the Variscan orogen have recently been considered to represent separate terranes [e.g., *Matte et al.*, 1990; *Pharaoh*, 1999; *Franke*, 2000; *Winchester and the PACE TMR Network Team*, 2002] usually correlated with Armorica and interpreted to form the Armorican Terrane Assemblage (ATA) [*Tait et al.*, 2000].

[7] The northeast margin of the Bohemian Massif corresponds to the Sudetes (Figure 2). In a geological sense, the low-mountainous region of the Sudetes is connected to the southern part of the Silesian-Lusatian Plain to the north. The boundary between these two regions of the Sudetes is the prominent Sudetic boundary fault, a Cenozoic feature rejuvenating an older Variscan fracture zone. In a tectonic context, the Sudetes comprise the Sudetic Mountains to the south and the Fore-Sudetic Block to the north. The entire Sudetic area extends between the WNW–ESE trending Odra Fault Zone in the northeast and the parallel Elbe Fault Zone in the southwest (Figure 2). The Sudetes contain a mosaic of variously metamorphosed volcano-sedimentary successions and igneous suites of pre-Carboniferous age. These metamorphic rocks are onlapped by Late Devonian to Carboniferous clastics that were deposited in intramontane troughs and intruded by voluminous, mostly late to post orogenic Carboniferous granites. The Sudetes, together with the entire Bohemian Massif, belong to an extensive belt of uplifts variably elevated during the latest Cretaceous to Cenozoic in response to the buildup of Alpine collision-related intraplate compressional stresses, rifting and mantle plume activity [e.g., *Ziegler*, 1990; *Dèzes et al.*, 2004].

[8] To the northeast along the Odra fault zone, the uplifted Sudetic internides are juxtaposed against the Variscan external thrust-and-fold belt that subcrops below the thick Permo-Mesozoic succession of the Fore-Sudetic Monocline [e.g., *Mazur et al.*, 2006]. The Variscan basement extends below the sedimentary cover as far north as the Dolsk fault (Figure 2) that defines at depth a boundary with the TESZ [*Grad et al.*, 2002a]. The Dolsk fault represents a major seismic discontinuity cutting across the upper and middle crust [e.g., *Guterch et al.*, 1986, 1992; *Grad et al.*, 2002a]. A subvertical orientation of the Dolsk fault indicated in these seismic refraction interpretations is not necessarily its real geometry, which also could be a thrust fault. The Variscan crust to the southwest of the Dolsk fault is in general 32–35 km thick [e.g., *Wilde-Piórko et al.*, 2005] with a two-layer seismic structure characterized by low *P* wave velocities down to the Moho discontinuity (<6.7 km s^{-1}) [*Grad et al.*, 2002a; *Majdański et al.*, 2006]. The exception is the southwest Bohemian Massif that is crossed by the S01 profile and contains high velocities in the

range of 6.8–7.0 km s^{-1} [*Enderle et al.*, 1998; *Hrubcová et al.*, 2005, 2008].

[9] A prominent feature of the western Bohemian Massif sampled by the S01 profile is the Eger (Ohře) rift that parallels the NE–SW oriented contact of the Saxothuringian zone with the Teplá-Barrandian and Moldanubian zones (Figure 2). The profile intersects the rift near its southwest boundary running approximately parallel to its trend. The geodynamically active area of the Eger rift belongs to the European Cenozoic rift system now [e.g., *Prodehl et al.*, 1995; *Dèzes et al.*, 2004]. Similarly its initiation and development were related to the Alpine collision in Late Cretaceous times. The Eger rift is characterized by an anomalous upper mantle structure, a thinned crust, abundant intraplate basaltic volcanism, seismicity, mantle-derived fluids approaching the surface, and a classical graben morphology associated with graben related sedimentary basins [*Špičk et al.*, 2005; *Plomerová et al.*, 2007].

3. Previous Geophysical Investigations in the Study Area

[10] The eastern part of the Variscan belt and its surroundings has been a target for several national geophysical projects in Germany, the Czech Republic and Poland, as well as large international projects. Crustal structure was previously investigated mainly with seismic experiments using different techniques: refraction/wide-angle reflection profiles [e.g., *Beránek and Dudek*, 1972; *Guterch et al.*, 1986, 1992; *Enderle et al.*, 1998; *Aichroth et al.*, 1992; *Blundell et al.*, 1992; *Mayerová et al.*, 1994; *Grad et al.*, 2002a, 2003a; *Málek et al.*, 2001; *Hrubcová et al.*, 2005, 2008; *Majdański et al.*, 2006, 2007; *Růžek et al.*, 2003, 2007; *Brückl et al.*, 2007], surface waves [e.g., *Neunhöfer et al.*, 1981; *Wielandt et al.*, 1987, 1988; *Novotný et al.*, 1995, 1997; *Malinowski*, 2005], reflection profiles [*DEKORP Research Group*, 1988, 1994; *DEKORP and Orogenic Processes Working Groups*, 1999; *Tomek et al.*, 1997; *Malinowski et al.*, 2007], and receiver functions [e.g., *Kind et al.*, 1995; *Geissler et al.*, 2005; *Wilde-Piórko et al.*, 2005].

[11] On the basis of the results of refraction profiles, the crust of the Bohemian Massif is 30–40 km thick, thickening gradually from the northwest (Saxothuringian Zone) to the southeast (Moldanubian Zone) [e.g., *Beránek and Dudek*, 1972; *Enderle et al.*, 1998; *Hrubcová et al.*, 2005, 2008]. However, the depth to the Moho has a local maximum beneath the Sudetes Mountains (about 35 km depth for the central Sudetes) and another in the southern part of the massif (about 40 km). The P wave seismic velocities of the crystalline upper crust are less than 6.0 km s^{-1} at the surface and increase to ~6.4 km s^{-1} down to a depth of about 15 km. The lower crust is characterized by P wave velocities of 6.6–7.1 km s^{-1}. The crustal thickness of the Paleozoic platform in Poland varies from 30 to 32 km beneath the Fore-Sudetic Monocline, to 30–35 km beneath the Fore-Sudetic Block and Sudetes Mountains [e.g., *Guterch et al.*, 1986, 1992; *Majdański et al.*, 2006].

[12] Independent crustal models for the eastern part of the Variscan belt were obtained using the receiver function technique for permanent seismological stations in Germany, the Czech Republic and Poland. Three different techniques, namely, 1-D inversion, forward modeling of Vs velocity, and simultaneous determination of Moho depth and Poisson's ratio in the crust, gave very consistent results [*Geissler et al.*, 2005; *Wilde-Piórko et al.*, 2005]. The crustal thickness obtained from these studies for the Bohemian Massif fits the Moho depth obtained from P wave analysis of refraction profiles well. However, the receiver function technique mainly constrains the S wave velocity distribution in the crust and, thus, complements controlled source profiles in which P waves are primarily recorded with S waves being weak or absent [e.g., *Wilde-Piórko et al.*, 2005].

[13] The shallowest Moho is found at 28–32 km depth in the Saxothuringian zone along the Czech-German border. A characteristic feature for this area is a strong increase of S wave velocities from the surface to a depth of about 5 km, on average from 3.3 to 3.7 km s^{-1}. In the depth interval 10–15 km, low velocities (~3.4 km s^{-1}) similar to those near the surface were detected. However, considering typical shear wave velocity distributions in the crust, the high velocities at ~5–10 km depth are those that are anomalous. In the central part of the Bohemian Massif, the Moho depth is slightly deeper (about 33–34 km), and the crust is more homogeneous. The crustal thickness in the southern and eastern parts of the Bohemian Massif is greater and reaches 35–40 km [*Wilde-Piórko et al.*, 2005]. A general feature of the receiver function study is that in the depth interval of 20–30 km, a systematic velocity increase is observed from ~3.5 to ~4.0 km s^{-1}. The velocity in the uppermost mantle is 4.6–4.7 km s^{-1}, however in the Saxothuringian zone the velocity begins to decrease at depths of 35–45 km.

[14] Earthquakes in Western Bohemia–Vogtland have been the subject of many studies, particularly the micro-earthquake swarm zone in the area of Nový Kostel [e.g., *Horálek et al.*, 1996, 2000; *Špičk et al.*, 1999; *Fischer and Horálek*, 2000, 2003; *Neunhöfer and Meier*, 2004; *Ibs-von Seht et al.*, 2006]. The Western Bohemia–Vogtland region is the southeastern part of the Saxothuringian earthquake province, which is an isolated area of active intraplate seismicity. Between 1962 and 1998 more than 17,000 earthquakes, mostly clustered in time and space, were detected with magnitude M_L from about −1.5 to 4.6. All epicenters are concentrated in a north to south striking belt about 100 km in length and 50 km in width. The last significant and well studied earthquake swarms occurred in 1985–1986, 1997 and 2000 in the Western Bohemia–Vogtland area. The 1997 Nový Kostel swarm occurred in the vicinity of the southwestern end of S01 and was located on a southwest dipping fault segment that intersects the Eger rift in a NNW–SSE direction [*Neunhöfer and Meier*, 2004] approximately midway between shotpoints SP41050 and SP41080 (Figure 1). During the large swarm in 1985–1986, the hypocentral volume of all the events was restricted to only about 2 km × 3.5 km × 1 km. The hypocentral volumes of the less intense events of the swarm in January of 1997 was even smaller and did not exceed 0.8 km × 1 km × 1 km [*Neunhöfer and Güth*, 1989; *Fischer and Horálek*, 2000]. The focal depth range of events in the Nový Kostel swarm is between 6 and 11 km, and in the other parts of the Western Bohemia–Vogtland area, focal depths reach up to 23 km [*Fischer and Horálek*, 2003].

[15] The gravity field of the Bohemian Massif has a regional background of between −40 and −60 mGal. A maximum between −10 and +10 mGal is observed in the

Table 1. Information on Seismic Shots Along the S01 Profile From the SUDETES 2003 Experiment[a]

Shot	Longitude °E	Latitude °N	Height Above Sea Level (m)	Date	Time UTC	Charge (kg)	Profile Distance (km)	Lateral Offset, (km)
41010	11.239200	49.654200	410	5 Jun 2003	0600:56.485	1400	−1.820	0
41020	12.078970	49.850670	470	4 Jun 2003	1711:25.649	1000	64.611	0
41021	12.080360	49.850640	450	5 Jun 2003	1427:00.000	935	64.703	0
41040	12.542615	49.977600	640	4 Jun 2003	1909:59.526	400	100.767	0
41050	12.222886	50.119815	540	4 Jun 2003	1709:59.525	400	88.392	−22.4
41060	12.776166	50.113666	690	4 Jun 2003	1809:59.476	400	122.128	−4.7
41061	12.908558	50.020931	620	5 Jun 2003	1909:59.569	400	127.057	7.7
41070	12.983333	50.133000	670	4 Jun 2003	2009:59.311	400	136.532	0
41080	12.668401	50.261005	510	5 Jun 2003	2109:59.546	400	123.449	−22.9
41090	13.278666	50.356166	320	4 Jun 2003	2209:59.575	400	166.265	−9.9
41100	14.065166	50.579333	350	4 Jun 2003	2309:59.329	400	227.284	−4.2
41110	14.396391	50.707368	130	6 Jun 2003	0009:59.789	400	254.606	−3.5
41120	15.133666	50.942750	350	5 Jun 2003	0109:59.328	400	312.780	0
41130	15.491969	51.155583	230	4 Jun 2003	2220:00.000	100	345.893	0
41140	16.034777	51.392980	120	5 Jun 2003	2220:00.000	250	391.718	0
41150	16.907244	51.743350	70	6 Jun 2003	0210:00.000	150	463.440	0
41160	18.584100	52.479008	70	6 Jun 2003	2250:00.000	250	603.437	0
42070	15.601655	50.903508	420	5 Jun 2003	0210:00.000	50	340.950	25.8
44040	13.635666	50.697000	730	4 Jun 2003	1900:00.624	400	207.476	−29.9
44050	13.687163	50.548466	280	4 Jun 2003	1849:59.990	400	201.974	−13.8
44060	14.282000	50.378666	200	4 Jun 2003	1920:00.689	400	232.765	24.4

[a]Longitude and latitude coordinates in WGS84; height of seismic source above sea level in m; lateral offset of shot is positive to the right side of the distance axis (toward SE) and negative to the left side (toward NW).

southern Moldanubian zone, and another between −20 and −10 mGal lies along the Eger rift, in the distance range of 80–200 km along the S01 profile. In the Sudetes, the anomaly is again between −20 and −10 mGal and the adjacent area to the northeast is characterized by near zero to positive anomalies of about +10 mGal. Farther to the northeast in the TESZ, the Bouguer anomaly reaches about −50 mGal, and is approximately zero within the adjacent EEC [*Grabowska and Raczyńska*, 1991; *Krysiński et al.*, 2000; *Królikowski and Petecki*, 1995; *Bielik et al.*, 2006; *Wybraniec*, 1999].

[16] While the gravitational field pattern of the Bohemian Massif is divided into positive and negative regional bands, the magnetic field pattern is considerably more complex due to the occurrence of local sources that disturb the regional character of the anomalous magnetic field. In the Bohemian Massif, along the southeastern edge of the Saxothuringian zone, the regional positive magnetic anomaly has a source in a deeper structure and produces a negative correlation of magnetic and gravity fields. In this case, the magnetic source is interpreted to occur under granite bodies. The belt of regional magnetic anomalies can be interpreted as an indication of volcano-plutonic magmatic activity in the Saxothuringian zone during Variscan [*Dallmeyer et al.*, 1995]. Also (U)HP granulites and eclogites as well as bodies of ultramafic rocks associated with the SE contact of the Saxothuringian zone locally contribute to the magnetic image, e.g., at the boundary with the Teplá-Barrandian zone [*Banka et al.*, 2002].

[17] The highest positive magnetic anomalies (>500 nT) are found in the neovolcanics in the Eger rift that lies along the Saxothuringian/Moldanubian contact. There, we may assume the presence of extensive subvolcanic intrusive bodies that are probably extensively differentiated and primarily basic intrusive complexes [*Dallmeyer et al.*, 1995; *Bucha and Blížkovský*, 1994; *Pokorný and Beneš*, 1997].

[18] Along the Polish part of the S01 profile between the Sudetes and TESZ, magnetic anomalies are subdued (±100 nT), and probably result from deeply buried magnetic basement. In contrast farther to the northeast within the EEC, magnetic anomalies vary from −1500 to +1500 nT and have short wavelengths due to the shallow basement. These anomalies express tectonic features and intrusive bodies within the Precambrian basement that is covered by 1–2 km of sediments [*Karaczun et al.*, 1978; *Petecki et al.*, 2003].

[19] Heat flow along the S01 profile ranges between 50 and 80 mW m^{-2}, which is relatively high for continental areas [*Čermák and Bodri*, 1998]. The lowest value of 50–60 mW m^{-2} occurs in the southwesternmost section of the profile in the Saxothuringian zone, and in the distance range of 80–250 km, high values (>70 mW m^{-2}) are found in the Eger rift region [*Lenkey et al.*, 2002]. It should be noted that along line parallel to the S01 profile some 20–30 km to the northwest, the heat flow is higher by 10–20 mW m^{-2}, reaching values about 90 mW m^{-2}. Between 300 and 400 km along the profile in the Sudetes Mountains region, heat flow again decreases to 50–60 mW m^{-2}. At 500 km along the profile near the southwest edge of the Polish basin, heat flow is about 75 mW m^{-2}. Farther to northeast beyond the termination of the profile, in the transition from the Trans-European suture zone (TESZ) to the East European craton (EEC), the heat flow value drops to about 40 mW m^{-2}. In general, the TESZ separates "cold" EEC lithosphere with low heat flow to the northeast from "hot" lithosphere in the Paleozoic terranes to the southwest [*Čermák et al.*, 1989; *Bruszewska*, 2001; *Majorowicz et al.*, 2003; *Lenkey et al.*, 2002].

4. Seismic Data: Acquisition, Processing, and Wavefield

[20] The field layout of the SUDETES 2003 seismic experiment is shown in Figure 1. This experiment was concentrated in the Czech Republic and Poland but also

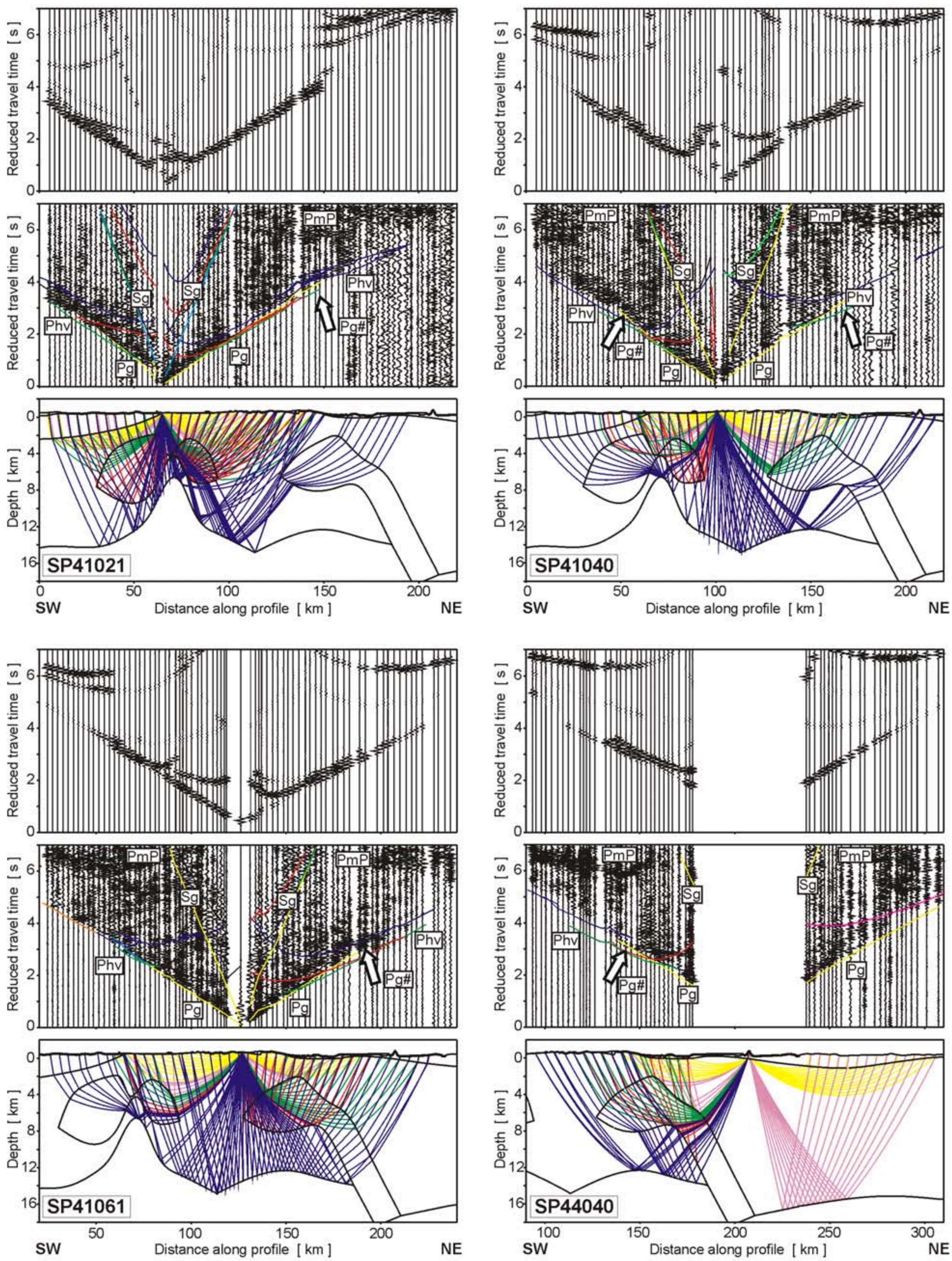
Reduced travel time [s]
Depth [km]
Distance along profile [km]
SW
NE
PmP
Sg
Phv
Pg
Pg#
SP41021
SP41040
SP41061
SP44040

Figure 3

covered portions of Germany, Hungary, and the Slovak Republic. The S01 profile is 630 km long with 21 shotpoints. Nearly half of the shotpoints were located exactly on the profile line, but logistic issues resulted in some shots being shifted up to ~30 km off the profile. The shots along the profile with their numbers are shown at the bottom of Figure 1, and detailed information about the shots is presented in Table 1. Although there were considerable variations due to local conditions and national procedures, the standard shooting configuration was to drill 5–10 boreholes to a depth of ~30–40 m and place 30–50 kg of explosives in each hole.

[21] About 200 single-channel recorders were deployed along the S01 profile with average spacing of 2.7 km in Germany and the Czech Republic, and 4.0 km in Poland. All recorders were of the "Texan" (RefTek 125, Refraction Technology, Inc.) type and employed 4.5 Hz vertical geophones. The sampling rate was 0.01 s, and the recording time window was 300 s for each shot. All shots in Poland were fired by a GPS-controlled blasting device. For the others, the shot instant was provided by placing a "Texan" seismic recorder and geophone at a horizontal distance of 20 m to the nearest borehole.

[22] The field records were cut to a length of 100 s starting at zero reduced time for a reduction velocity of 8 km s^{-1}. Examples of the recorded wavefield for *P* and *S* waves are shown in Figures 3–8. The *P* wavefield on the record sections has a good signal-to-noise ratio for the *Pg* (refraction/diving wave in the upper crust) and the *PmP* (Moho reflection) phases. However, the other crustal phases were complex and therefore difficult to pick, particularly in the southwestern (Eger rift within the Bohemian Massif) and northeastern (TESZ) sections of the profile. Identification and correlation of seismic phases was done manually on a computer screen using software that provides flexibility in applying scaling, filters, and reduction velocities [*Zelt*, 1994; *Środa*, 1999].

[23] Examples of record sections for the upper crust in the Eger rift area (about 100–220 km along the profile) are shown in Figure 3 together with calculated travel times, synthetic seismograms, and ray diagrams for the final velocity model. This area is not representative of the remainder of the profile because the observed wavefield changes significantly between shotpoints. Clear arrivals of refracted and reflected *P* waves from the crystalline crust are observed at up to 40–80 km offset (Figure 3, and SP41020 to the northeast in Figure 4). The termination of the *Pg* and *Sg* phases is abrupt and marked by $Pg^{\#}$ and corresponding $Sg^{\#}$. These phases are followed by others with higher apparent velocities (about 6.5 km s^{-1} for *P* waves) marked in the record sections as *Phv* and *Shv* (Figure 3). Our preferred explanation for this phenomenon is the presence of high-velocity bodies (HVB) in the upper crust. Very complex structures could also produce a match to the observed arrivals, but there is no evidence for such a situation in the Eger rift area. In the case of SP41061 to the southwest, the *Pg* phase traveling through HVBs is well recorded up to offsets of about 100 km. The *Pg* phase north of the Sudetes Mountains and in the TESZ is recorded up to offsets of 120–150 km (e.g., SP41150 in Figure 4 and SP41140 to the southeast in Figure 5) with an apparent velocity in the range 5.8–6.1 km s^{-1}.

[24] Examples of the full wavefield including both *P* and *S* waves are shown for three shots in Figure 4. Figure 5 (top) shows record sections from both ends of S01 that illustrate differences in the wavefields recorded in the Bohemian Massif and TESZ, and although *Pn* wave arrivals have almost the same reduced travel time (about 7 s for a reduction velocity 8 km s^{-1}), the sections differ significantly in the vicinity of the source. For the TESZ (SP41160 and the adjoining shotpoint SP41150), waves from the sedimentary cover (*Psed*) are observed up to offsets over 10 km. Also shown in Figure 5, the record section for SP41140 shows good quality *P* waves along the whole profile.

[25] As shown in Figures 3, 5 and 7, midcrustal reflections are observed all along S01, but they differ in amplitude, shape of signal and configuration relative to the *Pg* first arrival travel time and the *PmP* reflection. Also, *P* and *S* wave reflections from the Moho for some areas are observed as a strong short pulse (e.g., in distance range 180–220 km for SP41020 in Figure 5). In other areas, they form relatively long signals, 1–1.5 s for *PmP* (e.g., in distance range 270–350 km for SP41140 in Figure 5), and about 2 s for *SmS*, or they are very weak (e.g., in distance range 450–500 km for SP41160 in Figure 5). Strong *PmP* and *SmS* phases are observed in the southern part of the profile (Figure 4), while in the north they are not so distinct. In some cases, it is difficult to correlate the *PmP* phase because of strong reflections from the lower crust. At long offsets, well-developed overcritical crustal phases (P_{crustal}) are observed up to 200–250 km offsets. However, specific phase correlations for this group are not possible, and their travel times are represented only by envelope of high-amplitude arrivals (Figures 4 and 5).

[26] The Moho refractions (*Pn*) were not strong but where clear enough for confident correlation in several record sections (e.g., SP41061 and SP41150 in Figure 4), they are observed as first arrivals starting from 130 to 150 km offset, which indicates the Moho is at a depth of 30–35 km. As shown by earlier studies in the neighboring areas of the TESZ and EEC, the crossover distance between crustal *Pg* and mantle *Pn* refractions is much larger, about 200–220 km,

Figure 3. Four examples of the upper crust modeling in the area of Eger rift for SP41021, SP41040, SP41061 and SP44040. The "empty gap" for SP44040 is due to lateral shift of this shotpoint from the profile line by ~30 km. For each shotpoint, (top) synthetic seismograms, (middle) the amplitude normalized record section with theoretical travel times, and (bottom) the ray diagram calculated for the model (see Figure 6) using the SEIS83 ray-tracing technique are shown. A 2–15 Hz band-pass filter has been applied. *Pg*, *Sg*, *P*, and *S* waves refracted from the upper crust; $Pg^{\#}$ with arrow shows locations of abrupt terminations of the *Pg* wave related to high-velocity bodies in the uppermost crust; *Phv*, travel times of *P* waves refracted in a high-velocity body (*Vp* ~ 6.5 km s^{-1}); *PmP*, reflected waves from the Moho. Reduction velocity is 8.0 km s^{-1}.

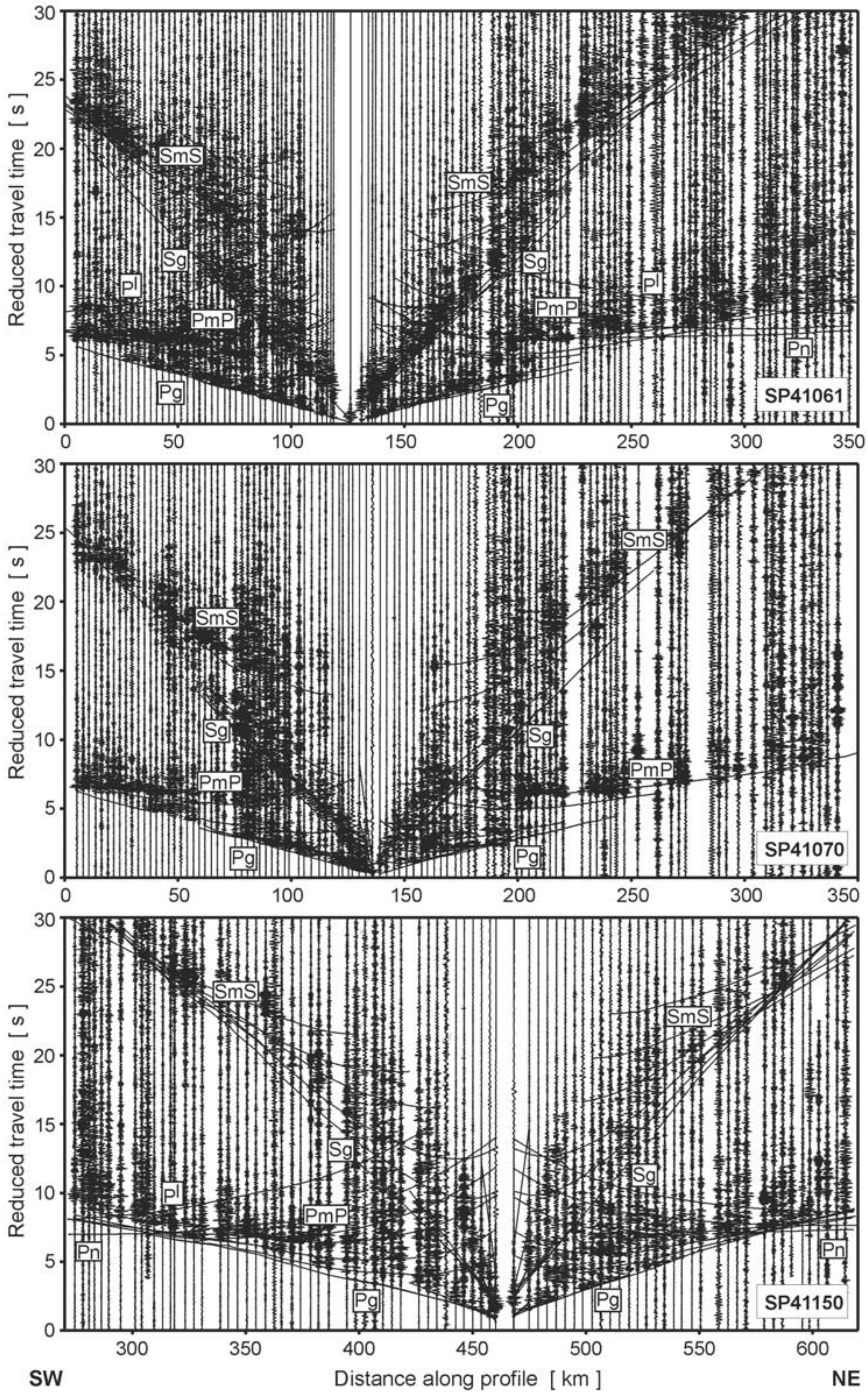

Figure 4. Amplitude-normalized seismic record sections for SP41061, SP41070, and SP41150 showing the full wavefield, including both *P* and *S* waves with theoretical travel times calculated for the lithospheric velocity model (see Figure 6) derived using the SEIS83 ray-tracing technique. A 1–10 Hz band-pass filter has been applied. *Pg*, *Sg*, *P*, and *S* waves refracted from the upper crust; *PmP*, *SmS*, waves reflected from the Moho; *Pn*, *Sn*, refracted waves from the Moho; P^{I}, waves from the lower lithosphere. Reduction velocity is 8.0 km s^{-1}.

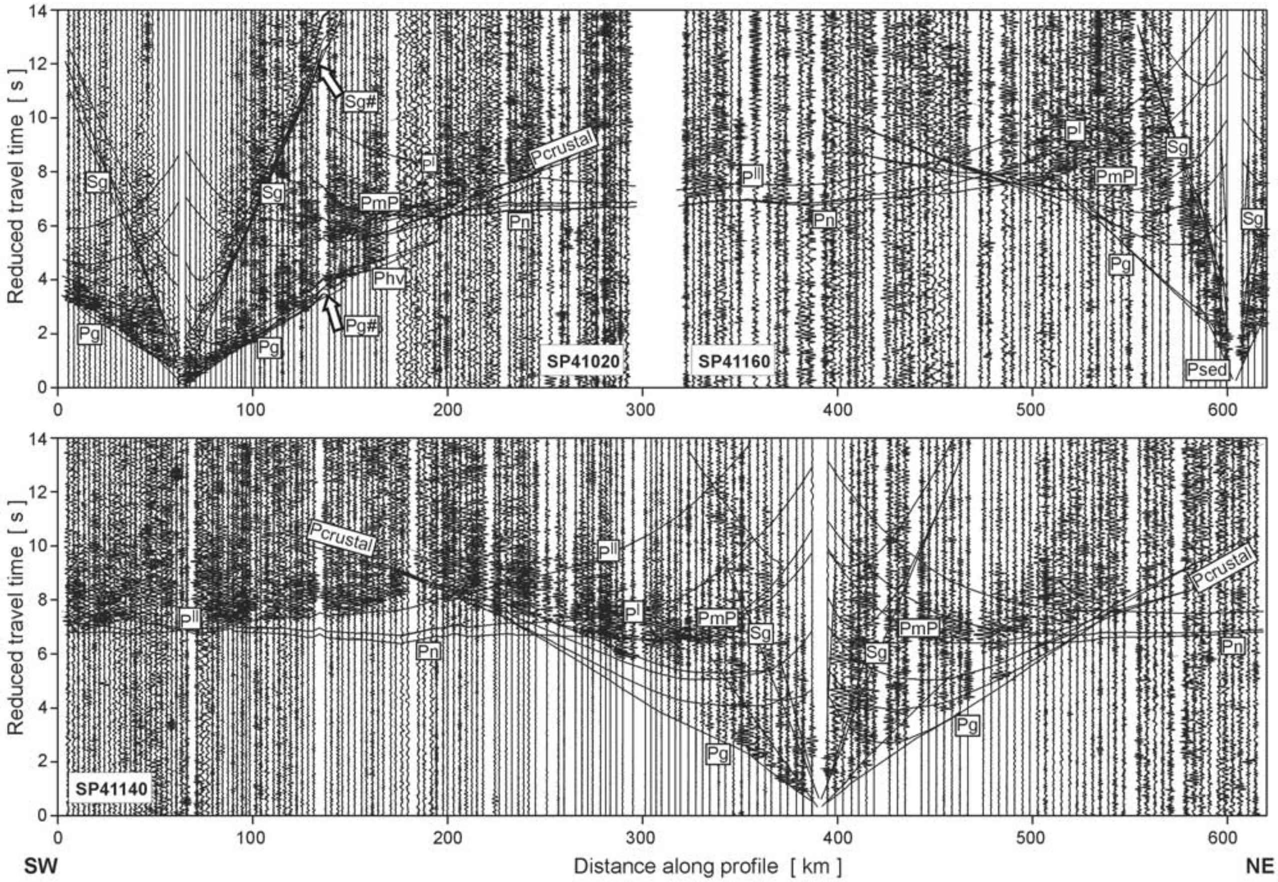

Figure 5. Amplitude-normalized seismic record sections for SP41020, SP41160, and SP41140 with theoretical travel times calculated for the lithospheric model (see Figure 6) derived using the SEIS83 ray-tracing technique. A 2–15 Hz band-pass filter has been applied. *Psed*, *P* waves in sediments; P_{crustal}, over critical crustal *P* waves traveling in the crust; P^{II}, waves from a sub-Moho boundary in the lower lithosphere; other seismic phases are described in Figures 3 and 4. Reduction velocity is 8.0 km s^{-1}.

indicating a much deeper Moho at 40–50 km [e.g., *Grad et al.*, 2003a, 2006]. The apparent velocities of *Pn* waves recorded along S01 are 7.9–8.0 km s^{-1}.

[27] Well-recorded mantle lithospheric waves (P^I and P^{II}) were observed only for large offsets from a few most effective shotpoints (e.g., SP41140 in Figure 5) and document lower lithospheric reflectors in the central part of the S01 profile. The best quality lower lithospheric phases were recorded from SP41140 to the south, up to 400 km offset (Figure 5). In some other record sections, lithospheric phases were also observed (e.g., SP41160 to the south, Figure 5; SP41150 and SP41061, Figure 4).

[28] In addition to the *SmS* reflection, other *S* wave phases were very well recorded for almost all shotpoints (Figure 4). In general better quality *S* waves are observed in the southern part of the profile (Bohemian Massif), while in the northern part (Sudetes and TESZ) they are usually lower quality and in a few cases were recorded only fragmentarily. *Sg* waves are usually well recorded up to offsets of 50–100 km and even more strongly imaged than *Pg* waves. It is interesting that termination points ($Sg^{\#}$) observed for *Sg* waves are in places almost identical to those for *Pg* waves. In most cases, the correlation of other *S* wave phases is impossible, and their travel times are represented by envelopes of high-amplitude arrivals.

5. Seismic Modeling of the Crust and Lower Lithosphere

[29] Detailed 2-D forward modeling of all refracted, reflected and postcritical phases identified in the correlation process was undertaken using ray-tracing techniques. The calculations of travel times, rays and synthetic seismograms were made using the ray theory package SEIS83 [*Červený and Pšenčík*, 1983] enhanced by employing the interactive graphical interfaces MODEL [*Komminaho*, 1997] and ZPLOT [*Zelt*, 1994] with modifications by *Środa* [1999]. Because of decades of geologic studies as well as petroleum and gas exploration, the initial model of the sedimentary cover and shallow basement in the Polish part of profile was constrained by borehole information and earlier geophysical studies, including high-resolution seismic reflection surveys (unpublished data of the oil and gas industry). This information provides a much more detailed model of the uppermost 5–10 km of sediments than can be obtained from the S01 profile refraction data alone. Using independent data to constrain the sedimentary cover, a preliminary generalized

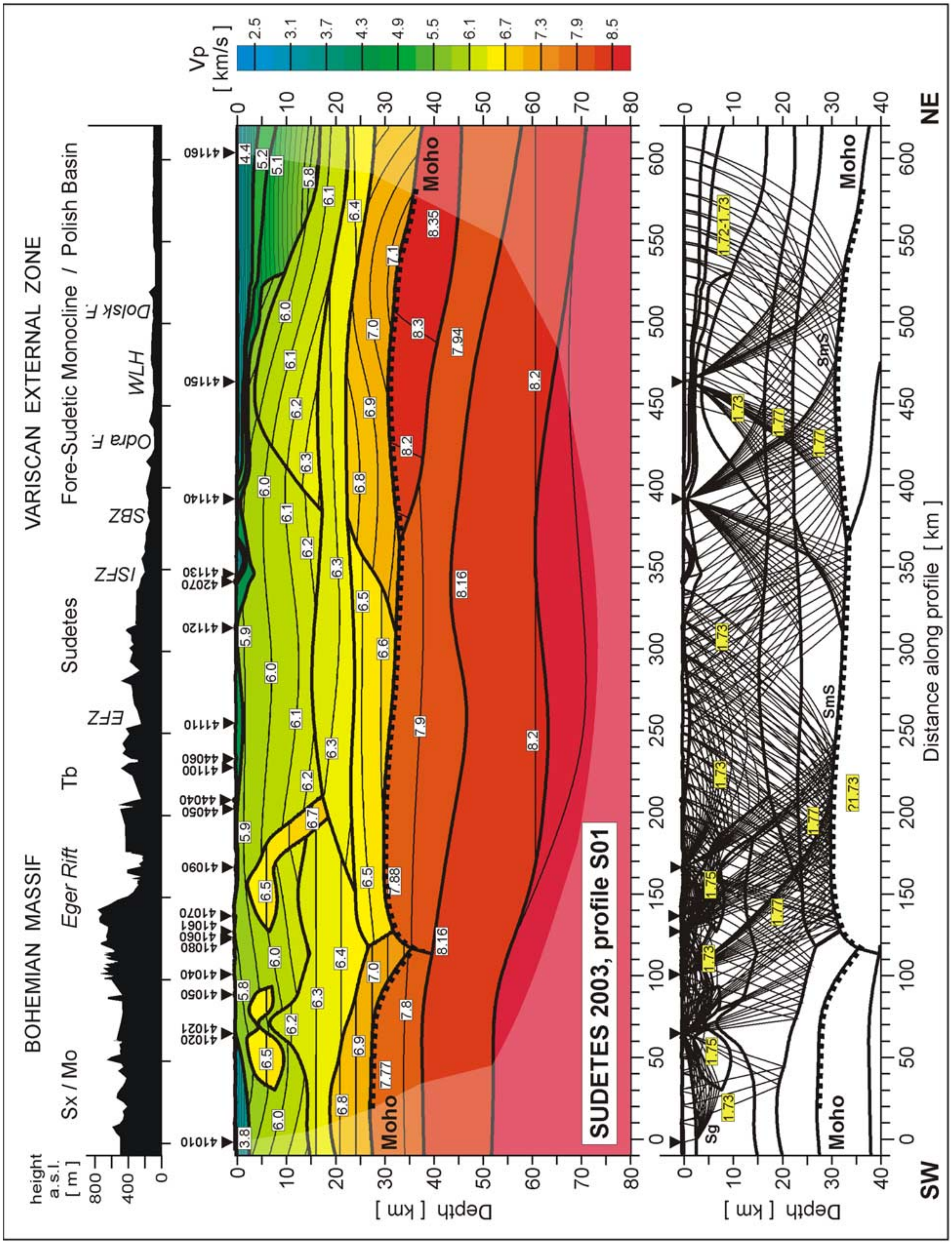
BOHEMIAN MASSIF
VARISCAN EXTERNAL ZONE
Sx / Mo
Eger Rift
Tb
EFZ
Sudetes
ISFZ
SBZ
Fore-Sudetic Monocline / Polish Basin
Odra F.
WLH
Dolsk F.
height a.s.l. [m]
Vp [km/s]
Depth [km]
Moho
SUDETES 2003, profile S01
SmS
Sg
Distance along profile [km]
SW
NE

Figure 6

model of the shallow structure was constructed that was only slightly adjusted (in the sense of seismic velocity and depth of boundaries) during the ray-tracing procedure. The overall velocity model for the S01 profile was successively altered by trial and error, and travel times were recalculated many times until agreement was obtained between observed and model-derived *P* wave travel times. Typical misfit for the observed and calculated *P* wave travel times was of the order of 0.1–0.2 s (Figures 3–5). Exceptionally good *Sg* and *SmS* waves were recorded for the area of the Bohemian Massif, where the *S* wavefield in fact repeats the *P* wavefield (Figure 4). However, even in this case, the phase correlation for corresponding *S* wave travel times was difficult. Therefore in the modeling of *S* waves, we used the geometry previously determined from *P* wave modeling, and by trial and error modeling fitted *S* wave arrivals by varying *Vp*/*Vs* for individual layers. Finally, in addition to kinematic modeling, synthetic seismograms were calculated to control velocity gradients within the layers and the velocity contrast at the seismic boundaries (Figures 3–5). The final synthetic seismograms show good qualitative agreement with the relative amplitudes of observed refracted and reflected *P* and *S* waves. The final lithospheric model derived for the structure along the S01 profile is shown in Figure 6 (vertical exaggeration is 3:1 for the model, and about 50:1 for topography). The model shows large variations in the internal structure of the crust, while the Moho topography along the 630 km long profile varies only in the relatively narrow depth interval of 28–35 km. Additionally, two reflectors were identified in the upper mantle at depths of ~45 and 65 km.

5.1. Model of the Structure

[30] Along the whole length of the S01 profile, a thin layer (a few 10s of m to ~100 m) of Tertiary and Quaternary sediments was inserted based mostly on geologic data, and a *Vp* of 1.6 km s^{-1} was assigned on the basis of earlier studies [*Grad*, 1991]. Within the Bohemian Massif, this layer covers the basement characterized by velocities in the range of 5.7–5.8 km s^{-1}. Only the southernmost margin of the Bohemian Massif (up to about 50 km of profile) is covered by 2 km of sedimentary rocks with velocities of 3.5–3.8 km s^{-1}. Significantly thicker sedimentary cover exists north of the Sudetes Mountains in Poland. For example in the vicinity of SP41130, a synclinal structure has a thickness of about 3 km. Apart from the Cenozoic layer, there occur extensive Mesozoic, Permian and older Paleozoic successions. The Permian layer (mostly Zechstein salt) plays an important role because of its high seismic velocities. In the depth range 2–7 km, Permian rocks are characterized by a *Vp* of 5.1–5.2 km s^{-1}, practically independent of depth (velocity gradient about 0.01 s^{-1}). The thickness of the Permian increases from 0.5 to 1 km at the northern margin of the Sudetes Mountains (about 350–400 km along profile) to 1.5–2 km in the TESZ (550–630 km of profile). The top of Permian dips toward the northeast from about 1 km north of the Sudetes Mountains to more than 6 km in the center of the Polish basin. In Mesozoic sediments, *Vp* increases with depth from about 3.4 km s^{-1} near surface to about 4.4 km s^{-1} at a depth of about 4 km. Consequently, the *Vp* velocity contrast at the Triassic–Permian boundary is near 1.5 km s^{-1}, creating a reflecting "screen" for seismic waves, particularly in near-vertical seismic reflection surveys. For this reason, the detailed seismic structure of the sub-Permian basement of the Polish basin is poorly known. The subsalt Paleozoic succession is characterized by a *Vp* of 4.9–5.8 km s^{-1} that is recorded at the maximum depth of about 17 km near the northeast termination of S01. The suspected crystalline basement below the Sudetes Mountains and Fore-Sudetic Monocline (distance 250–450 km along the profile) is characterized by a *Vp* of ~5.9 km s^{-1}, and the *Vp* of this unit is slightly higher (5.9–6.2 km s^{-1}) below the Polish basin. Very similar results were earlier obtained along the P4 and TTZ profiles in the TESZ [*Grad et al.*, 1999, 2003a; *Janik et al.*, 2005]. It should be noted that velocities in the basement beneath S01 are relatively low (*Vp* ~ 5.9 km s^{-1}) compared to those observed for the crystalline basement of the Precambrian EEC (*Vp* ~ 6.1–6.2 km s^{-1}).

[31] The *P* wave velocities within the deep basement of the Bohemian Massif were determined from *Pg* waves. In the area of the Eger rift, high-velocity bodies (HVB; *Vp* ~ 6.5 km s^{-1}) were recognized using *Phv* waves (Figure 3). These bodies exist in the crystalline upper crust from about 2–3 km down to about 10 km depth. The deep root of the HVB at 180–210 km along the profile is near the crossing point between S01 and Alp01 and was based on the velocity model for the Alp01 profile that included a similar body [*Brückl et al.*, 2007]. However, the S01 profile data alone are not sufficient to resolve this feature at depth. In general, it is difficult to constrain the velocity, thickness and shape of the HVBs. The top of the HVBs are well constrained from a few reciprocal branches of *Pg* and *Phv* phases (also from *Sg* and *Shv*), and particularly from termination points of refracted waves in the crystalline basement, $Pg^{\#}$ and $Sg^{\#}$. Their shapes appear to be complicated on the basis of variations in travel times for different shotpoints, particularly those laterally shifted from the profile line (Table 1). For example for SP41050 and SP41080 which are shifted 22 km northwest from the profile line, the record sections toward the northeast do not contain *Phv* phases, which is an indication of absence of a HVBs in this area. Together with the in-line shots, our pseudo 3-D interpretation of laterally shifted shots provides constraints on the lateral extent of the HVBs (Figure 8). The existence of HVBs in the Eger rift area is interpreted independently in a horizontal slice at

Figure 6. (middle) Two-dimensional *P* wave velocity model for SUDETES 2003 S01 profile obtained by forward ray-tracing modeling using SEIS83 package [*Červený and Pšenčík*, 1983]. The thick solid lines are layer boundaries, and thin lines are isovelocity contours in km s^{-1}; numbered triangles refer to shotpoints. Shaded areas at the bottom of model and in both lower corners show parts of the model that are not constrained by refracted and reflected waves (no ray coverage). (top) Topography along the profile is shown. (bottom) Crustal model with *Vp*/*Vs* ratio (in yellow boxes) and with *S* wave rays for shotpoints used in *Vp*/*Vs* ratio modeling. Vertical exaggeration is 3:1 for the lithospheric and crustal models and ~50:1 for topography.

10 km depth through a 3-D velocity model of the Bohemian Massif and Eastern Alps [*Behm et al.*, 2006, 2007].

[32] With the exception of the HVBs in the Eger rift area, the upper and middle crust along the S01 profile has velocities between 5.9 and 6.4 km s^{-1} (Figure 6). The lower crust is 7–10 km thick. On the basis of *Vp*, it can be divided into three regions: 6.8–7.0 km s^{-1} beneath the Bohemian Massif (up to 130 km distance along the profile); 6.5–6.6 km s^{-1} in the central portion of the profile (about 130–350 km), and 6.8–7.1 km s^{-1} in the TESZ region (from 350 km to the end of profile). Velocities of 6.5–6.6 km s^{-1} are typical of the majority of the Variscan belt of Europe. Velocities of 6.8–7.1 km s^{-1} are often referred as "high-velocity lower crust" (HVLC) and are typically observed beneath the TESZ and EEC [e.g., *Środa and POLONAISE P3 Working Group*, 1999; *Grad et al.*,

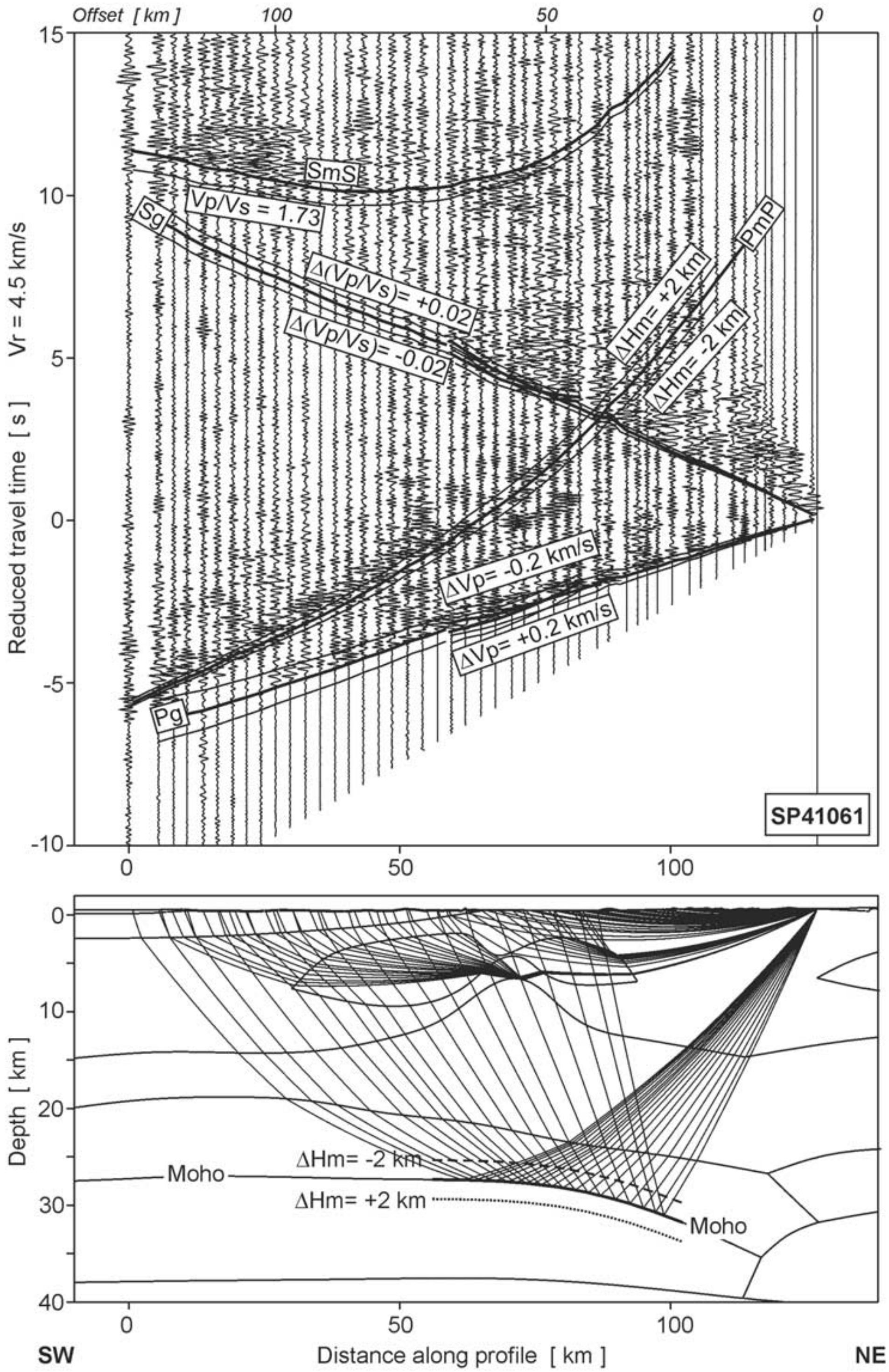

Figure 7

2002a] as well as beneath the southwest part of the Bohemian Massif [*Enderle et al.*, 1998; *Hrubcová et al.*, 2005, 2008].

[33] The velocity in the uppermost mantle determined from *Pn* wave travel times is about 7.8 km s^{-1} in the southwestern part of S01 beneath the Eger rift region, and about 7.9 km s^{-1} in its central part (Figure 6). In the northeastern part of S01 (~400 km to the end of profile), high velocities below the Moho (~8.3 km s^{-1}) were inserted on the basis of the crossing points with profiles P1 and TTZ [*Jensen et al.*, 1999; *Grad et al.*, 1999], where *Pn* arrivals are of very good quality. High velocities in the uppermost mantle beneath this part of S01 are confirmed by the northernmost shotpoint (SP41160; Figure 5). For this shotpoint, calculated *Pn* travel times at distances between 370 and 400 km fit the data well, but for a velocity of ~8 km s^{-1} the *Pn* travel times would arrive much too late (by about 0.7 s).

[34] The reflectors in the lower lithosphere are well resolved only in the central part of the S01 profile (distances between about 150 and 400–440 km), and they are about 15 and 30 km deeper than Moho. Similar lower lithosphere reflectors were also found in other areas of central Europe: in the TESZ [*Grad et al.*, 2002b, 2003a], the Bohemian Massif including the Sudetes Mountains [*Hrubcová et al.*, 2005; *Majdański et al.*, 2006], the Carpathians [*Grad et al.*, 2006; *Środa et al.*, 2006], and the Alps [*Brückl et al.*, 2007].

5.2. *Vp/Vs*: Results of *S* Wave Modeling

[35] The *S* wave modeling along S01 was performed by determining the *Vp/Vs* ratio for each layer using the final *P* wave seismic model (Figure 6) as a starting model for which the geometry and the *Vp* were not changed. We used this approach because the *S* wave travel time data alone were not sufficient for independent modeling of the *Vs* structure. By changing the *Vp/Vs* ratio by trial and error, we fitted theoretical *S* wave travel times to the observed ones. In the uppermost thin sedimentary layer, we assumed *Vp/Vs* = 1.83. In younger sediments at the southern margin of the Bohemian Massif and in the TESZ, the *Vp/Vs* ratio is 1.77. Deeper and older (Permian and lower Paleozoic) sediments in the TESZ are characterized by *Vp/Vs* values of 1.72 and 1.73, respectively. In the crystalline basement with *Vp* = 5.9–6.2 km s^{-1} (upper crust), the *Vp/Vs* ratio is 1.73. In the high-velocity bodies in the Eger rift region (*Vp* > 6.5 km s^{-1}), the corresponding *S* wave velocities are relatively low as indicated by a *Vp/Vs* = 1.75. These values were well determined from good quality *Pg* and *Sg* wave travel times. Since other *S* wave phase travel times were based on arrivals of an envelope of energy, they could not be employed for precise *Vp/Vs* determinations. However, if a standard value *Vp/Vs* = 1.73 is assumed for the deeper crust, the calculated *S* wave arrivals are early, and *Vp/Vs* = 1.77 fits the observed *S* wave travel times much better. Since we did not observe *Sn* waves, we can only speculate about the *Vp/Vs* ratio in the uppermost mantle. In the record section for SP41150 (TESZ part of the model), the amplitudes of *SmS* waves are small in relation to *PmP*, as well as to *SmS* waves within the Bohemian Massif. Thus, we can suggest that the relative *S* wave velocity contrast is significantly smaller than for *P* waves in the TESZ region. This effect could be caused by high *Vs* in the lower crust and/or low *Vs* in the uppermost mantle. For the calculation of synthetic seismograms a value of *Vp/Vs* = 1.73 was used.

5.3. Analysis of Accuracy, Resolution, and Uncertainties

[36] Uncertainties of velocity and depth in the model obtained using the ray-tracing technique result first of all from the uncertainties of subjectively picked travel times. Using modern techniques, the shot times and locations for shotpoints and receivers were measured very precisely, on the order 1 ms and few meters, respectively, with GPS systems, and these errors are insignificant in a crustal-scale experiment. On the other hand, uncertainties due to erroneous interpretation of arrivals cannot be estimated, but the probability of their accuracy increases with increasing quality and amount of data (number and effectiveness of shotpoints, signal-to-noise ratio, spacing between seismic stations, reciprocity of travel time branches, ray coverage in the model). In most cases, the ray-tracing technique used to model the picked travel times produced theoretical travel times that fitted the observed (experimental) travel times for both refracted and reflected waves with an accuracy of ±0.1–0.2 s. In addition, synthetic seismograms show good qualitative agreement with relative amplitudes of observed refracted and reflected waves.

[37] The following conclusions about the resolution and uncertainties of models derived from refraction and wide-angle reflection data are based in part on the experience we obtained from the POLONAISE'97 and CELEBRATION 2000 experiments, which were characterized by similar methodology, source and receiver density, and comparable data quality [e.g., *Janik et al.*, 2002; *Grad et al.*, 2003a, 2006]. For the S01 profile, we conducted sensitivity tests of the SEIS83 ray-tracing results calculated for *Pg*, *PmP*, *Sg* and *SmS* arrival times for SP41061 (Figure 7). Thick lines are travel times calculated for the final model shown in Figure 6. The arrival times of the *Pg* phase with the velocity perturbed

Figure 7. Test of resolution of calculated travel times using the SEIS83 ray-tracing technique for SP41061. Thick lines marked by *Pg*, *PmP*, *Sg*, and *SmS* arrival times are travel times calculated for the final model of the structure shown in Figure 6. The arrival times of the *Pg* phase with the velocity perturbed by +0.2 km s^{-1} and −0.2 km s^{-1} shown by lighter lines are significantly too early and too late in relation to recorded first breaks indicating that the velocity of the upper crust could be determined from the *Pg* wave with accuracy ±0.1 km s^{-1}. The arrival time of the *PmP* phase reflected from the Moho in the final model (~28 km depth) is shown together with arrival times with the depth perturbed by ±2 km marked by lighter lines. The sensitivity for estimation of the *S* wave velocity in the upper crust was tested using of the *Sg* phase with *Vp/Vs* perturbed by ±0.02. Early and late arrivals of the *Sg* phase are shown by lighter lines. Finally, the *SmS* phase reflected from the Moho calculated using the standard value *Vp/Vs* = 1.73 for the entire crust (lighter line) shows arrivals that are early by about 0.5 s, and the presence of relatively low *S* wave velocities in the crust (*Vp/Vs* is about 1.75–1.77). See text for more discussion. For this section a 2–15 Hz band-pass filter has been applied. Reduction velocity is 4.5 km s^{-1}.

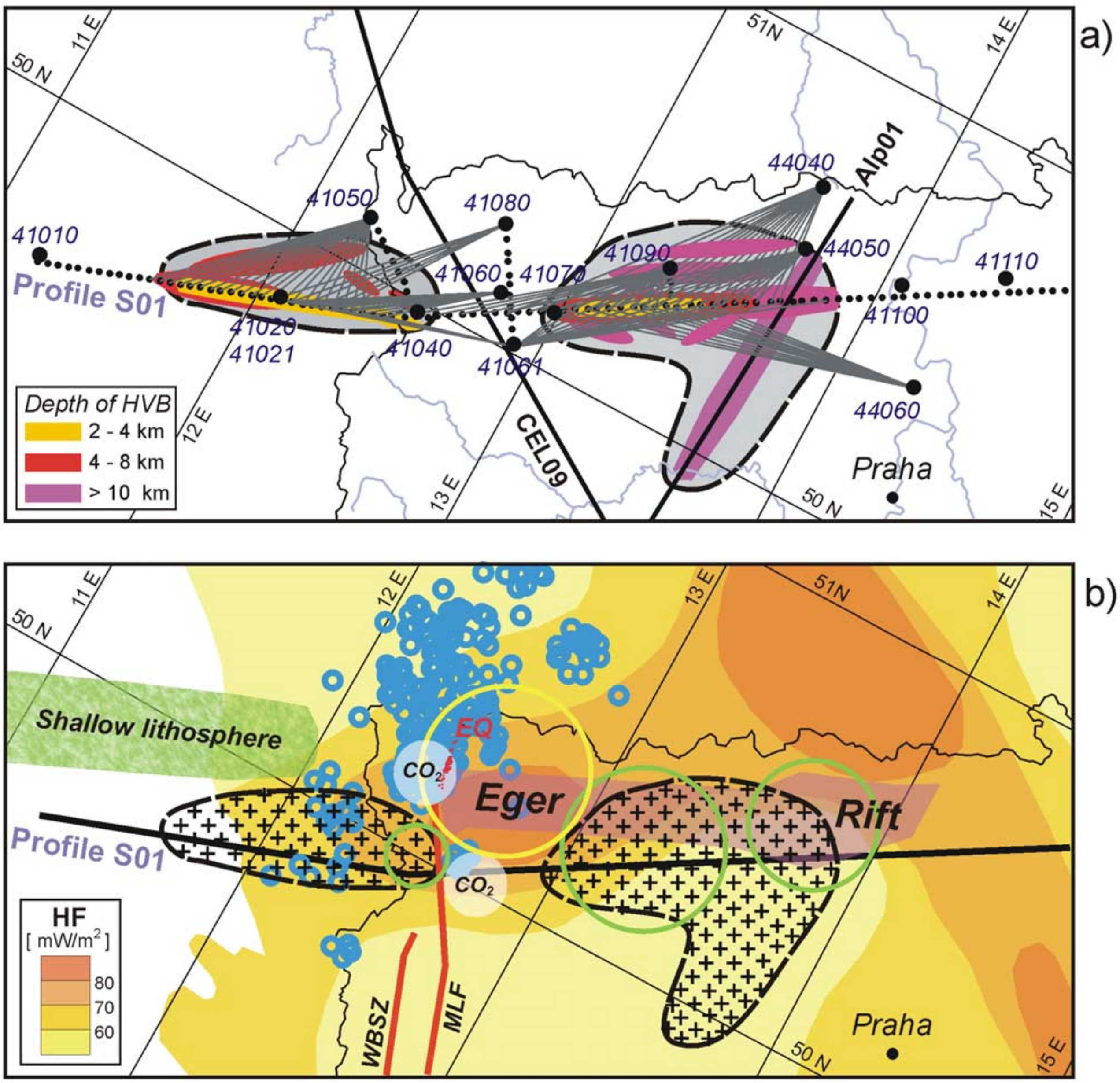

Figure 8. Summary of the pseudo 3-D seismic information in the vicinity of (a) S01 and (b) geophysical characteristics of the Eger rift area. In Figure 8a, colored areas show the high-velocity bodies (HVB) that were detected by the in-line shots and the off-line swaths, being colored according to depth of body. The HVB from the model of the Alp01 profile [*Brückl et al.*, 2007] is colored in a similar fashion. The lateral extent of the HVB was estimated using shotpoints located off of the S01 profile. It should be noted that the HVB was not found at profile CEL09 [*Hrubcová et al.*, 2005], which crosses the S01 profile just between the two bodies detected in this study. The interpreted extent of the high-velocity bodies is marked in gray in Figure 8a and by crosses in Figure 8b. In Figure 8b, a geophysical characteristics of the Eger rift area are shown on the background map of the surface heat flow [*Čermák*, 1977]; white circles are the distribution of CO_2 emanations [*Geissler et al.*, 2005; *Bräuer et al.*, 2005]; green circles show location of high-amplitude concentric magnetic anomalies related to Cenozoic volcanic activity [*Dallmeyer et al.*, 1995; *Šalanský*, 1996]; low-density granites [*Švancara et al.*, 2000] are marked by yellow circle. MLF, Mariánské Lázně Fault; WBSZ, West Bohemian Shear Zone. Blue open circles show location of the Western Bohemia–Vogtland earthquakes that are concentrated along the northwestern extension of the MLF. The microearthquake swarm zone is in the area of Novy Kostel (~12.5°E, ~50.2°N) and is marked as an EQ group of small red dots [*Fischer and Horálek*, 2000; *Ibs-von Seht et al.*, 2006]. The area of lithospheric thinning to about 80–90 km in the deep contact between the Saxothuringian and Moldanubian zones is delineated according to *Babuška and Plomerová* [2001].

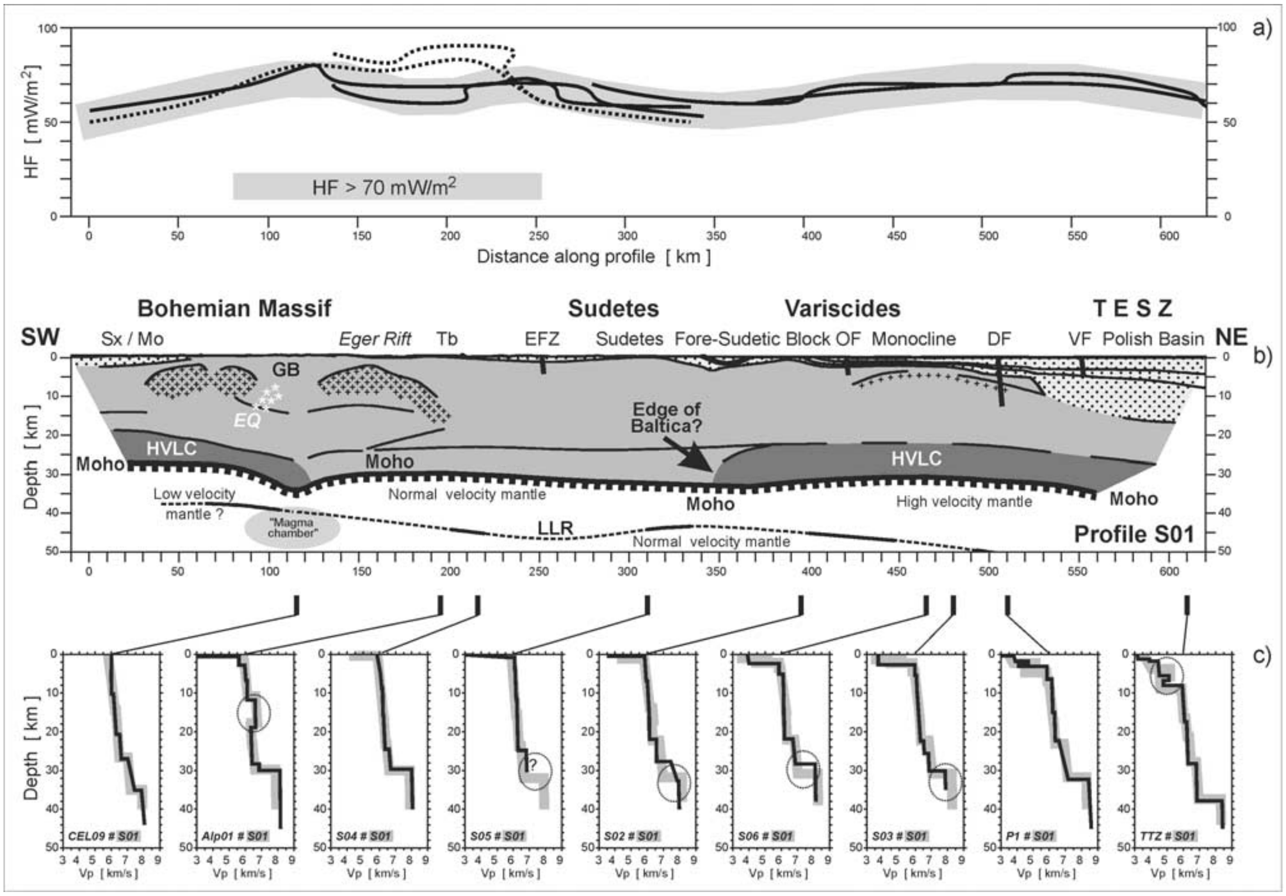

Figure 9. (b) Interpretative summary of lithospheric structure along the S01 profile. (a) Surface heat flow profiles [*Čermák*, 1977; *Lenkey et al.*, 2002; *Majorowicz et al.*, 2003; *Bruszewska*, 2001]. (c) A collection of *P* wave velocity models from other seismic profiles at their crossing points with S01. In Figure 9c, 1-D models from the S01 profile are shown by thick gray lines, and 1-D velocities for the CEL09, Alp01, S04, S05, S02, S06, S03, P1, and TTZ profiles are drawn as thin black lines [*Hrubcová et al.*, 2005; *Brückl et al.*, 2007; *Majdański et al.*, 2006; *Jensen et al.*, 1999; *Grad et al.*, 1999]. The locations of the crossing points are shown by thick vertical bars. Ellipses mark parts of the 1-D models that are discussed in detail in the text. DF, Dolsk fault; EFZ, Elbe fault zone; EQ and stars, microearthquake swarm zone in the area of Novy Kostel; GB, Karlovy Vary granite body in the upper crust; HVLC, high-velocity lower crust; LLR, lower lithospheric reflector; "Magma chamber," area of partial melting in the mantle under the Eger Rift; OF, Odra fault; VF, Variscan front.

by +0.2 km s^{-1} and -0.2 km s^{-1} shown by lighter lines are significantly too early and too late in relation to the recorded first breaks. This illustrates that the velocities in the upper crust can be determined from *Pg* waves with an accuracy of ±0.1 km s^{-1}, or even better locally. However, it should be remembered that these velocities are averages for regions of the crust with dimensions on the order of the recording station interval (2–4 km). In similar fashion, the arrival times of the *PmP* phase reflected from the Moho in the final model (~28 km depth) are shown together with arrival times with the depth perturbed by ±2 km, marked by lighter lines (Figure 7). The misfits for the distance range of 0 to 75 km (model coordinates) indicate that it is reasonable to claim that the Moho depth is resolved to at least ±2 km.

[38] The sensitivity for estimation of the *S* wave velocity in the upper crust was tested using the *Sg* phase with the *Vp*/*Vs* values in the model perturbed by ±0.02, and the early and late arrivals of *Sg* are shown by lighter lines (Figure 7). Finally, arrival times calculated for the *SmS* phase reflected from the Moho, using the standard value (*Vp*/*Vs* = 1.73) for the whole crust (lighter line), show arrivals that are early by about 0.5 s, and therefore indicate lower *S* wave velocities in the crust (*Vp*/*Vs* = 1.75–1.77). Thus, the uncertainty in *S* wave velocity, or rather *Vp*/*Vs* ratio, can be estimated as ±0.02 for the upper crystalline crust (from *Pg* and *Sg* waves), and as ±0.03 or more for deeper parts of the model where only envelopes of waves were correlated.

[39] In considering these estimates of uncertainty, the limitations of ray theory must be kept in mind. Also, our modeling was 2-D in nature and thus does not allow for the presence of out-of-plane refracted and reflected arrivals, which must be present to some extent in structurally complex areas such as the Eger rift and surroundings.

[40] Another way to assess uncertainty is through comparisons with other results in the region. In general, *P* wave velocities in the model for the S01 profile agree well with the models at crossing points with other recent profiles (Figure 1) [*Hrubcová et al.*, 2005, 2008; *Brückl et al.*, 2007;

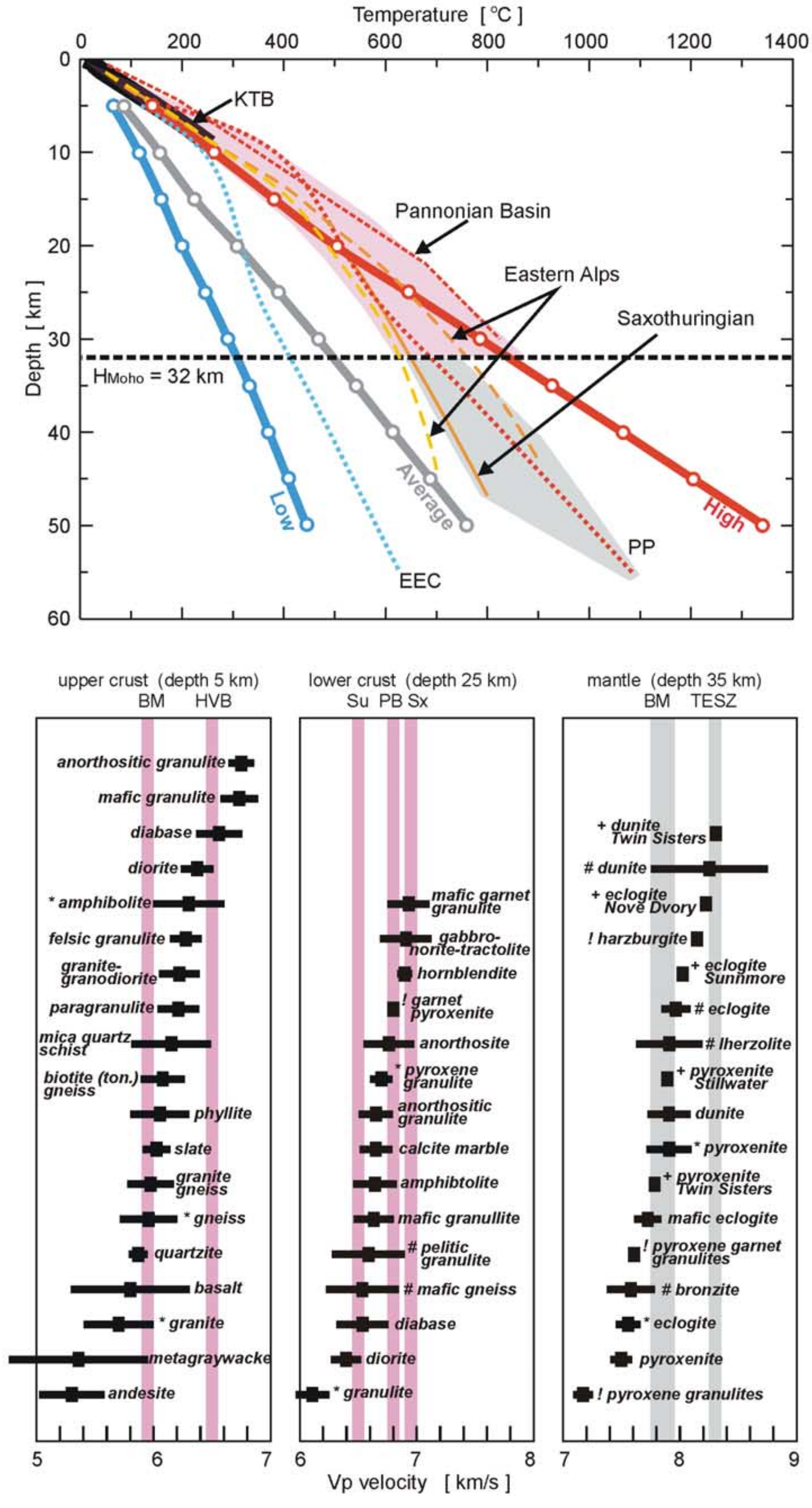
Temperature [°C]
0
200
400
600
800
1000
1200
1400
Depth [km]
KTB
Pannonian Basin
Eastern Alps
Saxothuringian
HMoho = 32 km
Low
Average
High
PP
EEC
upper crust (depth 5 km)
BM
HVB
anorthositic granulite
mafic granulite
diabase
diorite
* amphibolite
felsic granulite
granite-granodiorite
paragranulite
mica quartz schist
biotite (ton.) gneiss
phyllite
slate
granite gneiss
* gneiss
quartzite
basalt
* granite
metagraywacke
andesite
lower crust (depth 25 km)
Su
PB
Sx
mafic garnet granulite
gabbro-norite-tractolite
hornblendite
! garnet pyroxenite
anorthosite
* pyroxene granulite
anorthositic granulite
calcite marble
amphibtolite
mafic granullite
pelitic granulite
mafic gneiss
diabase
diorite
* granulite
mantle (depth 35 km)
BM
TESZ
+ dunite Twin Sisters
# dunite
+ eclogite Nové Dvory
! harzburgite
+ eclogite Sunnmore
# eclogite
# lherzolite
+ pyroxenite Stillwater
dunite
* pyroxenite
+ pyroxenite Twin Sisters
mafic eclogite
! pyroxene garnet granulites
bronzite
* eclogite
pyroxenite
! pyroxene granulites
Vp velocity [km/s]

Figure 10

Majdański et al., 2006; *Jensen et al.*, 1999; *Grad et al.*, 1999]. Velocity-depth (V-D) profiles were extracted from all of the models from earlier studies at their crossing point with S01 and are plotted in Figure 9 (dark lines) along with the corresponding S01 V-D profile (gray lines whose width indicate their approximate uncertainty). The areas circled on the V-D profiles are discussed in detail below.

[41] At the crossing point of Alp01 and S01, the high-velocity body at 12–18 km was constrained using data from the Alp01 profile. Data from S01 alone are not sufficient for modeling it to this depth. Thus, the match here is artificial to the extent that it is based on the integrated analysis of these two profiles. At the crossing points with profiles S05 and S02, the match is good down to the vicinity of the Moho, and the difference in the deep structure is due to the fact that the crossing point is near the ends of S05 and S02 (Figure 1) where the deep structure is poorly constrained. Profile S06 is relatively short so the uncertainty near the Moho is large, which suggests that the deep misfit is statistically insignificant. In the case of profile S03, the models differ only in uppermost mantle velocity. In this case, velocity along the S03 profile was constrained from a relatively short branch of the *Pn* wave [*Majdański et al.*, 2006]. For profile TTZ small differences occur in the sedimentary fill of the Polish basin due to the fact that we used detailed data from boreholes and shallow reflection seismic surveys that were not available at the time the TTZ profile was modeled [*Grad et al.*, 1999]. For crossing points with the remaining profiles (CEL09, S04, and P1) velocities from the S01 profile are essentially identical considering the uncertainties. Taking into account possible 2% anisotropy in the upper crust of the Bohemian Massif [e.g., *Vavryčuk et al.*, 2004; *Růžek et al.*, 2003], the differences at the crossing points in the southern portion of the S01 profile are small.

6. Discussion of Geological and Tectonic Implications

6.1. Crustal Lithologies

[42] We made an interpretation of crustal lithologies along the S01 profile based on the *P* wave velocities obtained by 2-D ray-tracing modeling (Figures 6 and 9b). We have inferred the most plausible lithologies along the profile by comparing modeled *Vp* values with global [*Christensen and Mooney*, 1995; *Weiss et al.*, 1999] and regional [*Christensen*, 1974; *Mueller*, 1995; *Grégoire et al.*, 2001] laboratory data for various rock assemblages. Lithological candidates for the upper crust, lower crust and uppermost mantle are shown in Figure 10. We used the temperature-depth curves for the low, average and high heat flow thermal regimes according to *Christensen and Mooney* [1995]. In the crust of the S01 profile region, the published temperature-depth curves for the Saxothuringian zone [*Čermák*, 1995], the Paleozoic platform in southwest Poland [*Majorowicz*, 1976], the Eastern Alps [*Vosteen et al.*, 2003], and the Pannonian basin [*Posgay et al.*, 2001] lie close to the high heat flow curve. This curve also fits the temperatures measured directly in the KTB borehole to a depth of about 9100 m [*Emmermann and Lauterjung*, 1997]. On the other hand, much lower temperatures are observed for the "cold" East European craton in northeast Poland [*Majorowicz*, 1976]. In the uppermost mantle (about 30–50 km depth), the temperatures inferred for the Saxothuringian zone and the Paleozoic platform are significantly lower than those for the high heat flow regime but significantly higher than for the average heat flow regime. Thus, for our comparison between seismic and laboratory data we used the "hot" regime for the crust (pink area in Figure 10) and the mean of the "hot/average" for the uppermost mantle (gray area in Figure 10).

[43] In Figure 10 (bottom), laboratory data for various rock assemblages are shown for a high-temperature regime in the crust (5 and 25 km depth) and for the mean described above for the uppermost mantle at 35 km depth [*Christensen and Mooney*, 1995; *Mueller*, 1995]. The original data of *Christensen* [1974], *Weiss et al.* [1999], and *Grégoire et al.* [2001] were corrected downward by 0.3 km s^{-1} to adjust for in situ temperature conditions. Shaded areas (pink and gray) represent modeled *Vp* velocities for the upper crust (5.95 km s^{-1} for the Bohemian Massif and 6.5 km s^{-1} for the HVB), lower crust (6.5 km s^{-1} for the Sudetes Mountains, 6.8 km s^{-1} for the Polish basin, and 6.95 km s^{-1} for the Saxothuringian zone), and uppermost mantle (7.8–7.9 km s^{-1} for the Bohemian Massif and 8.3 km s^{-1} for the TESZ) with

Figure 10. (top) Geothermal gradients and (bottom) comparison of the *Vp* velocities observed along S01 with laboratory data. As a reference, temperature-depth curves for three thermal regimes are shown for low, average, and high heat flow (thick blue, gray, and red lines with circles) according to *Christensen and Mooney* [1995]. For comparison, temperature-depth curves are shown for the area of the S01 profile: Saxothuringian [*Čermák*, 1995], Paleozoic Platform (PP) in southwest Poland [*Majorowicz*, 1976], and neighboring areas: "hot" Eastern Alps [*Vosteen et al.*, 2003] and Pannonian Basin [*Posgay et al.*, 2001], and "cold" East European craton (EEC) in northeast Poland [*Majorowicz*, 1976]. Thick black line extending to about 10 km shows measured temperature in KTB borehole [*Emmermann and Lauterjung*, 1997]. Shaded areas represent "hot" crust (pink) and "hot/average" mantle (gray) for the area close to the S01 profile. A dashed line at 32 km indicates the average Moho depth. Laboratory data for various rock assemblages are shown for high-temperature model in the crust at 5 and 25 km depth, and average/high-temperature model of the uppermost mantle at 35 km depth. Velocity values from laboratory data are plotted as crosses with black bars representing error estimates for the laboratory data. Anisotropy has been neglected. Most of the data are from *Christensen and Mooney* [1995]. Other data sources are indicated as follows: pluses, *Christensen* [1974]; asterisks, *Mueller* [1995]; number sign, *Weiss et al.* [1999]; and exclamation point, *Grégoire et al.* [2001]. Shaded vertical lines (pink and gray) represent modeled *Vp* velocities beneath the S01 profile: for the upper crust (5.95 km s^{-1} for the BM and 6.5 km s^{-1} for the HVB), for the lower crust (6.5 km s^{-1} for Sudetes Mountains, 6.8 km s^{-1} for Polish Basin, and 6.95 km s^{-1} for the Saxothuringian), and for the uppermost mantle (7.8–7.9 km s^{-1} for Bohemian Massif and 8.3 km s^{-1} for TESZ). The lines are shown with the estimated uncertainly of the velocity values of ±0.05 km s^{-1} in every case except for the upper mantle of the BM, where it is ±0.1 km s^{-1}.

an uncertainty of ±0.05 km s^{-1}. Bars represent published standard deviations for laboratory data. Anisotropy has not been taken into account, but it should be noted that in the vicinity of the crust-mantle transition, anisotropy can reach values from 1 to 5% (e.g., igneous rocks, quartzite, felsic granulite, eclogite) to 10–20% (e.g., phyllite, slate, amphibolite) and for single mineral crystals, even 30% (e.g., olivine, orthopyroxene, clinopyroxene) [e.g., *Christensen and Mooney*, 1995].

[44] The high-velocity bodies (HVBs) in the upper crust at a depth of 4–10 km near the Eger rift (Figure 6) have *P* wave velocities typical of diabase, diorite, or amphibolite. Since the HVBs lie along the boundary between the Saxothuringian and Teplá-Barrandian zones, it seems likely that these bodies were originally in the lower crust and were brought into the upper crust during the assembly of the terranes in this region. The HVBs can have originated either through "subduction erosion" and subsequent underplating of parts of the Saxothuringian plate or by intracrustal plug flow of overheated material [*Krawczyk et al.*, 2000]. Nevertheless, it cannot be ruled out that HVBs represent mafic intrusions in the rift zone comparable to those recognized beneath the Ethiopian rift [e.g., *Daly et al.*, 2008]. This possibility is, however, not supported by a relatively low Vp/Vs ratio (∼1.75) within the HVBs.

[45] Besides the HVBs, the upper crust throughout the Bohemian Massif shows velocities typical of gneisses, which are actually the most common lithology exposed in that area. The velocity model for the metamorphic upper crust between the Odra and Dolsk fault zones corroborates the available borehole data from the Wolsztyn-Leszno high testifying to the occurrence of phyllites in the basement of the sedimentary succession. A slightly higher-velocity layer (6.0–6.3 km s^{-1}) below 4–5 km depths may represent plutonic bodies and/or gneissic thrust sheets in the orogenic wedge of the external Variscan zone. The anomalous low-velocity upper crust of the TESZ can be interpreted as an extensive pile of low-grade metasediments (e.g., metagraywackes [*Grad et al.*, 2002a]). Alternatively, it may also represent a gneiss complex if intense NW–SE oriented anisotropy is assumed [*Jarosiński and Dąbrowski*, 2006] consistent with the regional geological context.

[46] The lower crust of the Bohemian Massif mostly consists of *P* wave velocities characteristic of pelitic granulites and/or mafic gneisses to mafic granulites as well as diabases (Figure 10). These lithologies are predictable in that area and essentially agree with the rock inventory found in exhumed tectonic units of lower crustal derivation. The velocity model cannot unequivocally resolve the characteristics of the lower crust at the contact of the Moldanubian and Saxothuringian zones. Two lithologies (mafic garnet granulite and a gabbro-norite-troctolite) (Figure 10) fit the velocity model equally well. The latter lithology is supported by findings of gabbro-noritic xenoliths in the Quaternary volcanics of the western Eger rift zone [*Geissler et al.*, 2007, and references therein]. A gabbro-noritic suite can be considered an important component of Proterozoic lower crust or the product of Paleozoic magmatic underplating. The same dilemma generally concerns the lower crust underlying the TESZ and Fore-Sudetic Monocline.

[47] The high-velocity upper mantle below the TESZ and the Fore-Sudetic Monocline is probably composed mostly of dunite as indicated by experimental data. In contrast, the upper mantle of the Bohemian Massif may potentially show more variable composition including pyroxenite, dunite and lherzolite. Thus, it significantly differs from the highly depleted upper mantle of the TESZ. Importantly, the velocity model does not support large-scale eclogitization of the mantle below the Bohemian section of the Variscan belt.

6.2. Geological Interpretation and Plate Tectonic Model

[48] The particular geological interest connected with the S01 profile emerges from the fact that this seismic line crosscuts a contact between the TESZ and the easternmost segment of the Variscan belt. This boundary is interpreted to separate the early Paleozoic Avalonian or Baltica-derived terranes accreted to the EEC margin in the northeast from the late Paleozoic collage of the Armorican terrane assemblage (ATA) in the southwest. Profile S01 extends across a number of geological units including from SW to NE: (1) the Moldanubian and Teplá-Barrandian zones of the Variscan belt, (2) the Sudetes at the northern margin of the Bohemian Massif, and (3) the Fore-Sudetic Monocline and the Polish trough in the area of the Paleozoic platform. Not all these units distinguished on the basis of shallow level geological observations are easy to identify by means of deep seismic refraction sounding. The seismic structure along the S01 profile allows discrimination of three major crustal domains: (1) the Moldanubian zone including the southeast margin of the Eger rift, (2) the Teplá-Barrandian zone jointly with the Sudetes, and (3) the TESZ as the basement of the Polish trough and the northern part of the Fore-Sudetic Monocline (Figures 2 and 6).

[49] The first 130 km of the profile is characterized by the occurrence of a high-velocity layer ($Vp > 6.8$–7.0 km s^{-1}) at the base of the crust (Figures 6 and 9). In the same distance interval, the profile follows the southern margin of the Eger rift that in turn follows the Variscan suture between the Saxothuringian and Moldanubian zones. The high-velocity layer is abruptly terminated at the boundary of the Teplá-Barrandian zone (Figure 6) which is defined at a shallower crustal level by the NW–SE oriented West Bohemian shear zone. Therefore, it remains indeterminate if the high-velocity layer is representative of the entire Saxothuringian crust as postulated by *Hrubcová et al.* [2005], underlies the Moldanubian zone in the vicinity of the Eger rift or is restricted to the rift zone itself. On both sides of the West Bohemian shear zone there occur high-velocity bodies in the upper crust of both the Moldanubian and Teplá-Barrandian zones (Figures 6 and 8). These bodies are located along the southern margin of the Eger rift, which corresponds to a Variscan suture between the Saxothuringian zone to the NW and the Moldanubian and Teplá-Barrandian zones to the southeast that has been identified on the basis of geological data [e.g., *Franke et al.*, 1995] and various geophysical methods [e.g., *Krawczyk et al.*, 2000]. Interestingly, we observe no HVBs in the area, where S01 intersects the West Bohemian Shear Zone and the deep-reaching pluton of the Karlovy Vary granite.

[50] The seismic structure is fairly uniform along the section of S01 that traverses the Teplá-Barrandian zone and the Sudetes (Figures 6 and 9). The resolution of the refraction method does not allow discrimination of smaller

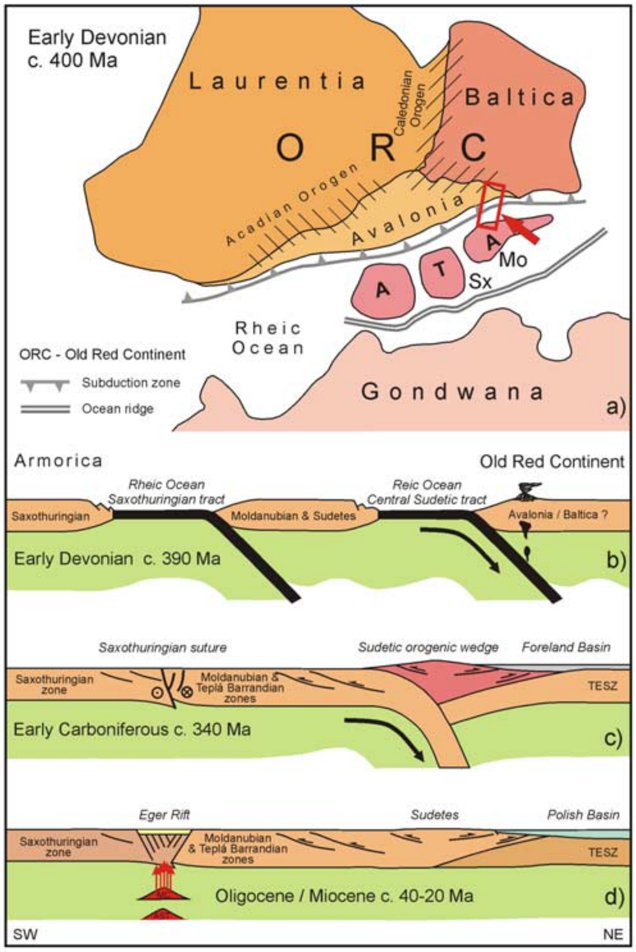

Figure 11. Geodynamic scenario for late Paleozoic accretion of the Variscan belt to the southwest margin of the TESZ. The paleogeographic sketch map (a) is inspired by the plate tectonic reconstructions of Ron Blakey (Northern Arizona University, http://jan.ucc.nau.edu/~rcb7/RCB.html). Box and arrow show area of the schematic cross sections (b–d); (b) branches of the Rheic Ocean are subducted northward beneath the Old Red Continent; Armorica-derived terranes are approaching the southwest margin of the TESZ; (c) Sudetic orogenic wedge is formed because of continental collision between the Armorican terranes and Old Red Continent; the Sudetic retrowedge is back thrust toward the N onto the plate margin containing the TESZ; the tectonic suture between the Saxothuringian and Moldanubian zones (terranes) is developed mostly as a result of highly oblique sinistral convergence; (d) the Eger rift is initiated along the preexisting Saxothuringian/Moldanubian suture. AST and MC, marked by red triangles areas of partial melting in the upper mantle ("magma chamber") and asthenosphere in the Eger rift; ATA, Armorican terrane assemblage; Mo, Moldanubian zone (terrane); Sx, Saxothuringian zone (terrane); TESZ, Trans-European suture zone.

crustal elements distinguished in this area based on geological evidence [*Matte et al.*, 1990; *Franke and Żelaźniewicz*, 2000, 2002; *Winchester and the PACE TMR Network Team*, 2002; *Aleksandrowski and Mazur*, 2002]. Therefore, the geological subdivision of the northern Bohemian Massif into smaller tectonostratigraphic units, if applicable, cannot be based on the present-day seismic velocity structure.

[51] The northern Variscan foreland represented by the TESZ concealed beneath the Polish basin has a seismic structure (Figure 6) that corresponds to the results of earlier surveys [*Grad et al.*, 2002a]. The innovative aspect of the S01 profile, regardless of the limitations of the refraction method, is the suggestion of gradual southward underthrusting of the TESZ lithosphere beneath the Variscan domain of the Bohemian Massif (Figure 6). The TESZ that corresponds to the southern margin of the Old Red Continent appears to be overridden from the south by the Variscan orogenic wedge reaching as far north beneath the Fore-Sudetic Monocline as the Dolsk fault (Figures 2 and 11). The high-velocity lower crust and upper mantle of the TESZ domain extend to the south up to the Odra fault zone and can be interpreted as the attenuated Baltica margin [*Grad et al.*, 2002a] or the edge of any other terrane potentially incorporated into the TESZ (e.g., magmatically underplated Avalonian lower crust [*Mazur and Jarosiński*, 2006], the Wielkopolska terrane of *Żelaźniewicz et al.* [2003], of the Kuiavia and/or Pomerania terranes of *Dadlez et al.* [2005]. Leaving the particularities of detailed terrane models still open, we interpret the upper crust of the Fore-Sudetic Monocline between the Odra and Dolsk fault zones (Figures 2, 6, 9, and 11) as part of a Variscan retrowedge back thrust toward the north onto the plate margin marked by the TESZ. This hypothesis is invoked from the reflectors/layer boundaries that dip to the southwest from about SP41150 in the upper crust and that bound the southern extent of the HVLC. The upper crust of the Fore-Sudetic Monocline has slightly higher velocity than upper crust of the Saxothuringian and Teplá-Barrandian (Figure 6). However, the Fore-Sudetic Monocline upper crust is noticeably different from that of the TESZ and, thus, probably belongs to the Variscan orogen.

[52] If the Variscan belt comprises elements of the Armorican terrane assemblage and the TESZ belongs to the former Old Red Continent [e.g., *Tait et al.*, 2000; *Franke*, 2000], the Sudetic area must contain the Rheic suture formed because of the late Paleozoic closure of the Rheic Ocean (Figure 11). The vestige of this suture [*Mazur et al.*, 2006] is still preserved in the Sudetes where there are occurrences of (U)HP rocks and an ophiolite complex. Subduction of the Rheic Ocean was probably northerly directed as postulated for the subduction of the Rheic domain beneath the Mid German Crystalline Rise [*Franke et al.*, 1995]. The northward polarity of subduction is supported by far-reaching deformation and metamorphism across the Bohemian Massif, feature indicative of the lower plate in a collision zone. Furthermore, the voluminous clastic input sourced within a continental volcanic arc is documented for the Variscan Carboniferous foreland basin onlapping the TESZ and concealed beneath the Permo-Mesozoic Polish basin [*Krzemiński*, 2005]. The geochemical affinity of sediments filling the Variscan foreland basin provides evidence for the volcanic arc established on the TESZ side of a collision zone probably above the subducted Rheic Ocean (Figure 11). The northward subduction of the Rheic Ocean beneath the Old Red Continent is supported by kinematic analysis of nappe complexes in southeast Germany [*Kroner and Hahn*, 2004; *Kroner et al.*, 2008]

and the occurrence of arc-related volcano-sedimentary successions in the eastern Sudetes [*Kalvoda et al.*, 2008; *Szczepański*, 2007].

[53] A significant imprint on the seismic velocity structure of the Bohemian Massif was produced by the formation of the Eger rift. A broad low-velocity anomaly in the upper mantle beneath the Eger rift was postulated by *Plomerová et al.* [2007] to represent an upwelling of the lithosphere-asthenosphere transition, providing a possible cause for the intraplate basaltic volcanism associated with the rift. The high-velocity bodies emplaced in the upper crust in the vicinity of the Eger rift could represent fragments of lower crustal units dismembered along a tectonic suture at the southeast contact of the Saxothuringian zone and thus could represent vestiges of the Saxothuringian tract of the Rheic Ocean subducted prior to the Variscan collision. Alternatively, the high-velocity bodies may represent basaltic intrusions since they crosscut the seismic velocity structure of the adjacent crust (Figure 6). If this is a case, the emplacent of the high-velocity bodies was probably connected with the Late Cretaceous–Cainozoic activity of the Eger rift. The initiation of the Eger rift along the Saxothuringian tectonic suture (Figures 11c and 11d) suggests Cenozoic reactivation of the preexisting Variscan weakness zone in response to Alpine collision-related intraplate compressional stresses [e.g., *Ziegler and Dèzes*, 2005]. This situation points to long-lived memory of the crust that is prone to reactivation of mechanically weakened structural discontinuities even after a long period of tectonic quiescence.

7. Summary

[54] The 630 km long S01 profile traverses the eastern part of the Variscan belt in central Europe between the Trans-European suture zone and the Precambrian east European craton in the north, and the Eastern Alps and Carpathians in the south. Good quality seismic data were interpreted using 2-D ray-tracing technique. The seismic model shows large variations in the internal structure of the crust (Figure 6), while the Moho topography varies in the relatively narrow depth interval of 28–35 km. In the southernmost margin of the Bohemian Massif (up to about 50 km along the profile) a near 2 km thick sedimentary sequence is characterized by Vp velocities 3.5–3.8 km s^{-1}. Significantly thicker sedimentary cover exists north of the Sudetes Mountains. In the TESZ concealed beneath the Polish basin, an anomalous low-velocity upper crust with $Vp < 6$ km s^{-1} down to about 17 km depth was found. The Permian layer in the depth range 2–7 km is characterized by Vp velocity 5.1–5.2 km s^{-1}, practically independent of depth. The top of the Permian strata dips toward the northeast from about 1 km north of the Sudetes Mountains to more than 6 km in the center of the Polish basin. In contrast to relatively low-velocity Mesozoic sediments (Vp increases with depth from about 3.4 km s^{-1} near surface, to about 4.4 km s^{-1} at depth of about 4 km) the velocity step at the Triassic–Permian boundary is near 1.5 km s^{-1}, creating a strong reflecting "screen" for seismic waves. Within the Bohemian Massif, a thin sedimentary layer covers the basement characterized by velocities in the range of 5.7–5.8 km s^{-1}. The suspected crystalline basement below the Sudetes Mountains and Fore-Sudetic Monocline (distance 250–450 km along the profile) is characterized by a Vp of ~5.9 km s^{-1}, while below the Polish basin Vp is slightly higher, 5.9–6.2 km s^{-1}. The basement velocities observed in the Variscan belt are low compared to those observed for the crystalline basement of the Precambrian EEC ($Vp \sim$ 6.1–6.2 km s^{-1} at depth about 1–5 km). In the area of the Eger rift, high-velocity bodies ($Vp \sim 6.5$ km s^{-1}) were recognized. They penetrate into the crystalline upper crust from about 2–3 km down to about 10 km depth. The pseudo 3-D interpretation of laterally shifted (off-line) shots recorded on the S01 profile constrain on the lateral extent of the HVBs (Figure 8). The upper and middle crust with velocities 5.9–6.4 km s^{-1} cover the 7–10 km thick lower crust which can be divided into three regions: 6.8–7.0 km s^{-1} beneath the southwestern part of the Eger rift (up to 130 km distance along the profile), 6.5–6.6 km s^{-1} in the central portion of the profile (about 130–350 km), and 6.8–7.1 km s^{-1} in the TESZ region (from 350 km to the end of profile). Velocities of 6.5–6.6 km s^{-1} are typical of the majority of the Variscan belt of Europe, while velocities of 6.8–7.1 km s^{-1} are often referred to as "high-velocity lower crust" (HVLC) and are typically observed beneath the TESZ and EEC (Figures 6 and 9). The three regions discussed above have Moho depths of 28–32, 30–33, and 30–35 km, respectively. The velocity in the uppermost mantle is about 7.8 km s^{-1} beneath the Saxothuringian and Moldanubian zones, and about 7.9 km s^{-1} in the central part of the S01 profile. In the northeastern part of S01 (~400 km to the end of profile), velocities below the Moho are relatively high, ~8.3 km s^{-1}. Additionally below the Moho, two reflectors were identified in the upper mantle at depths of about 45 and 65 km. In general, the seismic model for profile S01 shows good agreement at crossing points with other profiles made in this area (Figure 9c).

[55] Crustal and uppermost mantle velocities obtained in seismic modeling permit an interpretation of lithologies along the S01 profile. The anomalous low-velocity upper crust of the TESZ can be interpreted as an extensive pile of low-grade metasediments (e.g., metagraywackes). The high-velocity bodies ($Vp > 6.5$ km s^{-1}) emplaced in the upper crust at the depth of 4–10 km in the Eger rift area have velocities indicative of lower crustal rocks or mafic intrusions. The high seismic velocity of the upper mantle below the TESZ and the Fore-Sudetic Monocline indicates it is composed mostly of dunite. In contrast, the upper mantle of the Bohemian Massif may potentially show more variable composition including pyroxenite, dunite and lherzolite.

[56] Our seismic model enables us to recognize three major crustal domains: (1) the Moldanubian zone (border to Saxothuringian zone) beneath the southwestern part of the Eger rift, (2) the Teplá-Barrandian zone and the Sudetes, and (3) the TESZ in the basement of the Polish trough and the northern part of the Fore-Sudetic Monocline (Figures 2 and 6). Along the boundary (suture?) between the Saxothuringian and Moldanubian zones, the Eger (Ohře) rift that is an element of the European Cenozoic rift system reactivated this preexisting Variscan feature. The S01 profile images the TESZ crust as being onlapped by the Variscan orogenic wedge of the Sudetes. The deflection of the TESZ foreland plate under a tectonic load of the Variscan wedge explains the development of the Carboniferous foreland

basin presently buried beneath the southwestern portion of the Polish basin. At the same time, our seismic model supports the northward polarity of subduction of the Rheic Ocean below the margin of the Old Red Continent. Though no relics of a fossil subduction zone are preserved in the form of seismic reflectors, the northward subduction accounts for the widespread deformation and metamorphism of the lower plate comprised within the Bohemian Massif.

[57] **Acknowledgments.** The authors thank the SUDETES 2003 Working Group: M. Behm, T. Bodoky, R. Brinkmann, M. Brož, E. Brückl, W. Czuba, T. Fancsik, B. Forkmann, M. Fort, E. Gaczyński, W. H. Geissler, M. Grad, R. Greschke, A. Guterch, S. Harder, E. Hegedűs, A. Hemmann, P. Hrubcová, T. Janik, G. Jentzsch, G. Kaip, G. R. Keller, K. Komminaho, M. Korn, O. Korousová, M. Majdański, J. Málek, M. Malinowski, K. C. Miller, E.-M. Rumpfhuber, A. Špičák, P. Środa, E. Takács, T. Tiira, J. Vozár, M. Wilde-Piórko, J. Yliniemi, and A. Żelaźniewicz. It is only through the participation of approximately 200 individuals that the preparation, execution, and data processing for SUDETES 2003 could be successfully completed. It is not possible to acknowledge individually everyone from many technical staff and students. The University of Leipzig provided 25 instruments for this project. Sources of financial and infrastructure support are in Austria, Institute of Geodesy and Geophysics, Vienna University of Technology; in Czech Republic, Ministry of Environment of the Czech Republic; and in Finland, Finnish participation was based on a long-standing exchange between the Finnish and Polish Academies of Sciences; in Germany, German participation was supported by the Friedrich-Schiller-Universität, Jena and the Bundesanstalt für Geologie Wissenschaften und Rohstoffe; in Hungary, Eötvös Loránd Geophysical Institute; in Poland, Polish Oil and Gas Company, and Institutes of Geophysics of the Polish Academy of Sciences and the University of Warsaw through the Association for Deep Geological Investigations in Poland (ADGIP); in Slovak Republic, the Geological Survey and Academy of Sciences provided support; in the United States, direct funding was provided by the National Science Foundation (INT) and the Texas Higher Education Coordinating Board. IRIS/PASSCAL is supported by the U.S. National Science Foundation (NSF) and provided the majority of the instrumentation for this experiment, and most of these instruments were provided through grants to the University of Texas at El Paso (State of Texas Higher Education Coordinating Board, NSF/MRI, and the DOD). The authors are grateful to two referees, Charlotte Krawczyk and Peter Maguire, for helpful and exhaustive comments.

References

Aichroth, B., C. Prodehl, and H. Thybo (1992), Crustal structure along Central Segment of the EGT from seismic-refraction studies, *Tectonophysics*, *207*, 43–64, doi:10.1016/0040-1951(92)90471-H.

Aleksandrowski, P., and S. Mazur (2002), Collage tectonics in the northeasternmost part of the Variscan Belt: The Sudetes, Bohemian Massif, in *Palaeozoic Amalgamation of Central Europe*, edited by J. A. Winchester, T. C. Pharaoh, and J. Verniers, *Geol. Soc. Spec. Publ.*, *201*, 237–277.

Babuška, V., and J. Plomerová (2001), Subcrustal lithosphere around the Saxothuringian-Moldanubian Suture Zone—A model derived from anisotropy of seismic wave velocities, *Tectonophysics*, *332*, 185–199, doi:10.1016/S0040-1951(00)00255-9.

Banka, D., T. C. Pharaoh, J. P. Williamson, and the TESZ Project Potential Field Core Group (2002), Potential field imaging of Palaeozoic orogenic structure in northern and central Europe, *Tectonophysics*, *360*, 23–45, doi:10.1016/S0040-1951(02)00345-1.

Behm, M., F. Bleibinhaus, E. Brückl, M. Grad, S. Mertl, CELEBRATION 2000 Working Group, and ALP 2002 Working Group (2006), A new seismic model of the Eastern Alpine crust, paper presented at the First European Conference on Earthquake Engineering and Seismology (a joint event of the 13th ECEE & 30th General Assembly of the ESC), Eur. Assoc. of Earthquake Eng., Geneva, Switzerland, 3–8 Sept.

Behm, M., E. Brückl, W. Chwatal, and H. Thybo (2007), Application of stacking and inversion techniques to three-dimensional wide-angle reflection and refraction seismic data of the Eastern Alps, *Geophys. J. Int.*, *170*, 275–298, doi:10.1111/j.1365-246X.2007.03393.x.

Beránek, B., and A. Dudek (1972), The results of deep seismic sounding in Czechoslovakia, *Z. Geophys.*, *38*, 415–427.

Berthelsen, A. (1998), The Tornquist Zone northwest of the Carpathians: An intraplate-pseudosuture, *Geol. Foeren. Stockholm Foerh.*, *120*, 223–230.

Bielik, M., et al. (2006), Gravity anomaly map of the CELEBRATION 2000 region, *Geol. Carpathica*, *57*(3), 145–156.

Blundell, D., R. Freeman, and S. Mueller (Eds.) (1992), *A Continent Revealed: The European Geotraverse*, 275 pp., Cambridge Univ. Press, Cambridge, U.K.

Bräuer, K., H. Kämpf, S. Niedermann, and G. Strauch (2005), Evidence for ascending upper mantle-derived melt beneath the Cheb basin, central Europe, *Geophys. Res. Lett.*, *32*, L08303, doi:10.1029/2004GL022205.

Brückl, E., et al. (2003), ALP 2002 seismic experiment, *Stud. Geophys. Geod.*, *47*, 671–679, doi:10.1023/A:1024780022139.

Brückl, E., et al. (2007), Crustal structure due to collisional and escape tectonics in the Eastern Alps region based on profiles Alp01 and Alp02 from the ALP 2002 seismic experiment, *J. Geophys. Res.*, *112*, B06308, doi:10.1029/2006JB004687.

Bruszewska, B. (2001), 2D temperature and heat flow modeling for the Earth's crust profile LT-7, in *Lithosphere Structure From Deep Seismic Soundings Along LT-7 Profile and Rheology Modeling*, *Central Geol. Arch.*, no. 91/2002, edited by P. Krzywiec, 250 pp., Pol. Geol. Inst., Warsaw.

Bucha, V., and M. Blížkovský (Eds.) (1994), *Crustal Structure of the Bohemian Massif and the West Carpathians*, Academia Praha, Prague.

Čermák, V. (1977), Heat flow map of the Bohemian Massif, *J. Geophys.*, *42*, 455–488.

Čermák, V. (1995), A geothermal model of the Central Segment of the European Geotraverse, *Tectonophysics*, *244*, 51–55, doi:10.1016/0040-1951(94)00216-V.

Čermák, V., and L. Bodri (1998), Heat flow map of Europe revised, *Dtsch. Geophys. Ges. V.*, *II*, 58–63.

Čermák, V., J. Šafanda, and A. Guterch (1989), Deep temperature distribution along three profiles crossing the Teisseyre-Tornquist tectonic zone in Poland, *Tectonophysics*, *164*, 151–163, doi:10.1016/0040-1951(89)90009-7.

Červený, V., and I. Pšenčík (1983), SEIS83 - numerical modeling of seismic wave fields in 2-D laterally varying layered structure by the ray method, in *Documentation of Earthquake Algorithm*, edited by E. R. Engdahl, *Rep. SE-35*, pp. 36–40, World Data Cent. A for Solid Earth Geophys., Boulder.

Chaloupský, J., I. Chlupáč, J. Mašek, J. Waldhausrová, and J. Cháb (1995), Moldanubian region, Teplá-Barrandian zone, stratigraphy, in *Pre-Permian Geology of Central and Eastern Europe*, edited by R. D. Dallmeyer, W. Franke, and K. Weber, pp. 379–391, Springer, Berlin.

Christensen, N. I. (1974), Compressional wave velocities in possible mantle rocks to pressures of 30 kbars, *J. Geophys. Res.*, *79*, 407–412, doi:10.1029/JB079i002p00407.

Christensen, N. I., and W. D. Mooney (1995), Seismic velocity structure and composition of the continental crust: A global view, *J. Geophys. Res.*, *100*(B6), 9761–9788, doi:10.1029/95JB00259.

Czuba, W., M. Grad, U. Luosto, G. Motuza, V. Nasedkin, and POLONAISE P5 Working Group (2002), Upper crustal seismic structure of the Mazury complex and Mazowsze massif within East European craton in NE Poland, *Tectonophysics*, *360*, 115–128, doi:10.1016/S0040-1951(02)00352-9.

Dadlez, R. (1978), Sub-Permian rock complexes in the Koszalin-Chojnice Zone (in Polish with English summary), *Kwartalnik Geol.*, *22*(2), 269–301.

Dadlez, R. (2000), Pomeranian Caledonides (NW Poland), fifty years of controversies: A review and a new concept, *Geol. Q.*, *44*, 221–236.

Dadlez, R., M. Grad, and A. Guterch (2005), Crustal structure below the Polish Basin: Is it composed of proximal terranes derived from Baltica?, *Tectonophysics*, *411*(1–4), 111–128, doi:10.1016/j.tecto.2005.09.004.

Dallmeyer, R. D., W. Franke, and K. Weber (Eds.) (1995), *Pre-Permian Geology of Central and Western Europe*, 604 pp., Springer, New York.

Daly, E., D. Keir, C. J. Ebinger, G. W. Stuart, I. D. Bastow, and A. Ayele (2008), Crustal tomographic imaging of a transitional continental rift: The Ethiopian rift, *Geophys. J. Int.*, *172*, 1033–1048, doi:10.1111/j.1365-246X.2007.03682.x.

DEKORP and Orogenic Processes Working Groups (1999), Structure of the Saxonian Granulites: Geological and geophysical constraints on the exhumation of high-pressure/high-temperature rocks in the mid-European Variscan belt, *Tectonics*, *18*(5), 756–773, doi:10.1029/1999TC900030.

DEKORP Research Group (1988), Results of the DEKORP 4/KTB Oberpfalz deep seismic reflection investigations, *Geophys. J.*, *62*, 69–101.

DEKORP Research Group (1994), The deep seismic reflection profiles DEKORP 3/MVE-90, *Z. Geol. Wiss.*, *22*(6), 623–825.

Dèzes, P., S. M. Schmid, and P. A. Ziegler (2004), Evolution of the European Cenozoic rift system: Interaction of the Alpine and Pyrenean orogens with their foreland lithosphere, *Tectonophysics*, *389*, 1–33, doi:10.1016/j.tecto.2004.06.011.

Emmermann, R., and J. Lauterjung (1997), The German Continental Deep Drilling Program KTB: Overview and major results, *J. Geophys. Res.*, *102*(B8), 18,179–18,201, doi:10.1029/96JB03945.

Enderle, U., K. Schuster, C. Prodehl, A. Schulze, and J. Bribach (1998), The refraction seismic experiment GRANU95 in the Saxothuringian belt, southeastern Germany, *Geophys. J. Int.*, *133*, 245–259, doi:10.1046/j.1365-246X.1998.00462.x.

Fischer, T., and J. Horálek (2000), Refined locations of the swarm earthquake in the Nový Kostel focal zone and spatial distribution of the January 1997 swarm in Western Bohemia, Czech Republic, *Stud. Geophys. Geod.*, *44*, 210–226, doi:10.1023/A:1022162826079.

Fischer, T., and J. Horálek (2003), Space-time distribution of earthquake swarm in the principal focal zone of the NW Bohemia/Vogland seismoactive region: Period 1985–2001, *J. Geodyn.*, *35*, 125–144, doi:10.1016/S0264-3707(02)00058-3.

Franke, W. (2000), The mid-European segment of the Variscides: Tectonostratigraphic units, terrane boundaries and plate tectonics evolution, in *Orogenic Processes: Quantification and Modelling in the Variscan Belt*, edited by W. Franke et al., *Geol. Soc. Spec. Publ.*, *179*, 35–61.

Franke, W., and A. Żelaźniewicz (2000), The eastern termination of the Variscides: Terrane correlation and kinematic evolution, in *Orogenic Processes: Quantification and Modelling in the Variscan Belt*, edited by W. Franke et al., *Geol. Soc. Spec. Publ.*, *179*, 63–86.

Franke, W., and A. Żelaźniewicz (2002), Structure and evolution of the Bohemian Arc, in *Palaeozoic Amalgamation of Central Europe*, edited by J. Winchester, T. Pharaoh, and J. Verniers, *Geol. Soc. Spec. Publ.*, *201*, 279–293.

Franke, W., R. D. Dallmeyer, and K. Weber (1995), Geodynamic evolution, in *Pre-Permian Geology of Central and Eastern Europe*, edited by R. D. Dallmeyer, W. Franke, and K. Weber, pp. 579–593, Springer, Berlin.

Geissler, W. H., H. Kämpf, R. Kind, K. Klinge, T. Plenefisch, J. Horálek, J. Zedník, and V. Nehybka (2005), Seismic structure and location of a CO_2 source in the upper mantle of the western Eger (Ohře) rift, central Europe, *Tectonics*, *24*, TC5001, doi:10.1029/2004TC001672.

Geissler, W. H., H. Kämpf, W. Seifert, and P. Dulski (2007), Petrological and seismic studies of the lithosphere in the earthquake swarm region Vogtland/NW-Bohemia, central Europe, *J. Volcanol. Geotherm. Res.*, *159*, 33–69, doi:10.1016/j.jvolgeores.2006.06.011.

Grabowska, T., and M. Raczyńska (1991), Structure of the Earth's crust on the Polish Lowland in the light of gravimetric modelling, *Publ. Inst. Geophys. Pol. Acad. Sci.*, *A-19*(230), 85–110.

Grad, M. (1991), Seismic wave velocities in the sedimentary cover of the Palaeozoic platform in Poland, *Bull. Pol. Acad. Earth Sci.*, *39*(1), 13–22.

Grad, M., et al. (1999), Crustal structure of the Mid-Polish Trough beneath the Teisseyre-Tornquist Zone seismic profile, *Tectonophysics*, *314*, 145–160.

Grad, M., A. Guterch, and S. Mazur (2002a), Seismic refraction evidence for crustal structure in the central part of the Trans-European suture zone in Poland, in *Palaeozoic Amalgamation of Central Europe*, edited by J. A. Winchester, T. C. Pharaoh, and J. Verniers, *Geol. Soc. Spec. Publ.*, *201*, 295–309.

Grad, M., G. R. Keller, H. Thybo, A. Guterch, and the POLONAISE Working Group (2002b), Lower lithospheric structure beneath the Trans European Suture Zone from POLONAISE'97 seismic profiles, *Tectonophysics*, *360*, 153–168, doi:10.1016/S0040-1951(02)00350-5.

Grad, M., et al. (2003a), Crustal structure of the Trans-European suture zone region along POLONAISE'97 seismic profile P4, *J. Geophys. Res.*, *108*(B11), 2541, doi:10.1029/2003JB002426.

Grad, M., A. Špičák, G. R. Keller, A. Guterch, M. Brož, and E. Hegedűs (2003b), SUDETES 2003 seismic experiment, *Stud. Geophys. Geod.*, *47*, 681–689, doi:10.1023/A:1024732206210.

Grad, M., A. Guterch, G. R. Keller, T. Janik, E. Hegedűs, J. Vozár, A. Ślaczka, T. Tiira, and J. Yliniemi (2006), Lithospheric structure beneath trans-Carpathian transect from Precambrian platform to Pannonian basin: CELEBRATION 2000 seismic profile CEL05, *J. Geophys. Res.*, *111*, B03301, doi:10.1029/2005JB003647.

Grégoire, M., I. Jackson, S. Y. O'Reilly, and J. Y. Cottin (2001), The lithospheric mantle beneath the Kerguelen Islands (Indian Ocean): Petrological and petrophysical characteristics of mantle mafic rock types and correlation with seismic profiles, *Contrib. Mineral. Petrol.*, *142*, 244–259.

Guterch, A., M. Grad, R. Materzok, and E. Perchuć (1986), Deep structure of the Earths crust in the contact zone of the Palaeozoic and Precambrian platforms in Poland (Tornquist-Teisseyre Zone), *Tectonophysics*, *128*, 251–279, doi:10.1016/0040-1951(86)90296-9.

Guterch, A., et al. (1992), Laminated structure of the lower crust in the fore-Sudetic region in Poland, derived from seismic data, *Phys. Earth Planet. Inter.*, *69*, 217–223, doi:10.1016/0031-9201(92)90138-L.

Guterch, A., M. Grad, H. Thybo, G. R. Keller, and K. C. Miller (1998), Seismic experiment spreads across Poland, *Eos Trans. AGU*, *79*(26), 302, 305.

Guterch, A., M. Grad, H. Thybo, G. R. Keller, and the POLONAISE Working Group (1999), POLONAISE'97—International seismic experiment between Precambrian and Variscan Europe in Poland, *Tectonophysics*, *314*, 101–121, doi:10.1016/S0040-1951(99)00239-5.

Guterch, A., M. Grad, G. R. Keller, K. Posgay, J. Vozár, A. Špičak, E. Brückl, Z. Hajnal, H. Thybo, and O. Selvi (2000), CELEBRATION 2000: Huge seismic experiment in central Europe, *Geol. Carpathica*, *51*(6), 413–414.

Guterch, A., M. Grad, G. R. Keller, and CELEBRATION 2000 Organizing Committee (2001), Seismologists celebrate the new millennium with an experiment in central Europe, *Eos Trans. AGU*, *82*(45), 529, 534–535.

Guterch, A., M. Grad, A. Špičák, E. Brückl, E. Hegedűs, G. R. Keller, H. Thybo, and CELEBRATION 2000, ALP 2002, SUDETES 2003 Working Groups (2003a), An overview of recent seismic refraction experiments in central Europe, *Stud. Geophys. Geod.*, *47*, 651–657, doi:10.1023/A:1024775921231.

Guterch, A., M. Grad, G. R. Keller, K. Posgay, J. Vozár, A. Špičák, E. Brückl, Z. Hajnal, H. Thybo, O. Selvi, and the CELEBRATION 2000 Experiment Team (2003b), CELEBRATION 2000 seismic experiment, *Stud. Geophys. Geod.*, *47*, 659–669, doi:10.1023/A:1024728005301.

Hajnal, Z., E. Hegedűs, G. R. Keller, T. Fancsik, A. C. Kovács, and R. Csabafi (2004), Low-frequency 3-D seismic survey of upper crustal magmatic intrusions in the northeastern Pannonian basin of Hungary, *Tectonophysics*, *388*, 239–252, doi:10.1016/j.tecto.2004.05.007.

Horálek, J., F. Hampl, A. Boušková, and T. Fischer (1996), Seismic regime of the West Bohemian earthquake swarm region: Preliminary results, *Stud. Geophys. Geod.*, *40*, 398–412, doi:10.1007/BF02300767.

Horálek, J., J. Šílený, T. Fischer, A. Slancová, and A. Boušková (2000), Scenario of the January 1997 West Bohemia earthquake swarm, *Stud. Geophys. Geod.*, *44*, 491–521, doi:10.1023/A:1021811600752.

Hrubcová, P., P. Środa, A. Špičák, A. Guterch, M. Grad, G. R. Keller, E. Brueckl, and H. Thybo (2005), Crustal and uppermost mantle structure of the Bohemian Massif based on CELEBRATION 2000 data, *J. Geophys. Res.*, *110*, B11305, doi:10.1029/2004JB003080.

Hrubcová, P., P. Środa, and the CELEBRATION 2000 Working Group (2008), Crustal structure at the easternmost termination of the Variscan belt based on CELEBRATION 2000 and ALP 2002 data, *Tectonophysics*, doi:10.1016/j.tecto.2008.07.009, in press.

Ibs-von Seht, M., T. Plenefisch, and E. Schmedes (2006), Faulting style and stress field investigations for swarm earthquakes in NE Bavaria/Germany—The transition between Vogtland/NW-Bohemia and the KTB-site, *J. Seismol.*, *10*, 197–211, doi:10.1007/s10950-005-9008-5.

Janik, T., J. Yliniemi, M. Grad, H. Thybo, T. Tiira, and POLONAISE P2 Working Group (2002), Crustal structure across the TESZ along POLONAISE'97 seismic profile P2 in NW Poland, *Tectonophysics*, *360*, 129–152, doi:10.1016/S0040-1951(02)00353-0.

Janik, T., M. Grad, A. Guterch, R. Dadlez, J. Yliniemi, T. Tiira, E. Gaczyński, and the CELEBRATION 2000 Working Group (2005), Lithospheric structure of the Trans-European suture zone along the TTZ-CEL03 seismic transect (from NW to SE Poland), *Tectonophysics*, *411*, 129–155, doi:10.1016/j.tecto.2005.09.005.

Jarosiński, M., and M. Dąbrowski (2006), Rheological models of the lithosphere across the Trans-European suture zone in northern and western part of Poland (in Polish with English summary), *Prace Państwowego Inst. Geol.*, *188*, 143–166.

Jensen, S. L., T. Janik, H. Thybo, and the POLONAISE Working Group (1999), Seismic structure of the Palaeozoic platform along POLONAISE'97 profile P1 in southwestern Poland, *Tectonophysics*, *314*, 123–143, doi:10.1016/S0040-1951(99)00240-1.

Kalvoda, J., O. Babek, O. Fatka, J. Leichmann, R. Melichar, S. Nehyba, and P. Spacek (2008), Brunovistulian terrane (Bohemian Massif, central Europe) from late Proterozoic to late Paleozoic: A review, *Int. J. Earth Sci.*, *97*(3), 497–518, doi:10.1007/s00531-007-0183-1.

Karaczun, K., M. Karaczun, M. Bilińska, and A. Uhrynowski (1978), Magnetic map of Poland, scale 1:500,000, Pol. Geol. Inst., Warsaw.

Keller, G. R., and R. D. Hatcher Jr. (1999), Comparison of the lithospheric structure of the Appalachian–Ouachita orogen and Paleozoic orogenic belts in Europe, *Tectonophysics*, *314*, 43–68, doi:10.1016/S0040-1951(99)00236-X.

Kind, R., G. L. Kosarev, and N. V. Petersen (1995), Receiver functions at the stations of the German Regional Seismic Network (GRSN), *Geophys. J. Int.*, *121*, 191–202, doi:10.1111/j.1365-246X.1995.tb03520.x.

Komminaho, K. (1997), Software manual for programs MODEL and XRAYS—A graphical interface for SEIS83 program package, *Rep. 20*, 31 pp., Dep. of Geophysics Univ. of Oulu, Oulu, Finland.

Kossmat, F. (1927), Gliederung des varistischen Gebirgsbaues, *Abh. Sächsischen Geol. Landesamts*, *1*, 1–39.

Krawczyk, C. M., E. Stein, S. Choi, G. Oettinger, K. Schuster, H.-J. Götze, V. Haak, O. Oncken, C. Prodehl, and A. Schulze (2000), Geophysical constraints on exhumation mechanisms of high-pressure rocks: The Saxo-Thuringian case between the Franconian Line and Elbe Zone, in

Orogenic Processes: Quantification and Modeling in the Variscan Belt, edited by W. Franke et al., *Geol. Soc. London Spec. Publ.*, *179*, 303–322.
Królikowski, C., and Z. Petecki (1995), *Gravimetric Atlas of Poland*, Pol. Geol. Inst., Warsaw.
Kroner, U., and T. Hahn (2004), Sedimentation, Deformation und Metamorphose im Saxothuringikum während der variszischen Orogenese: Die komplexe Entwicklung von Nord-Gondwana während kontinentaler Subduktion und schiefer Kollision, *Geol. Saxonica*, *48/49*, 133–146.
Kroner, U., et al. (2008), Variscan tectonics, in *The Geology of Central Europe*, vol. 1, *Precambrian and Paleozoic*, edited by T. McCann, pp. 599–664, Geol. Soc., London.
Krysiński, L., M. Grad, and POLONAISE'97 Working Group (2000), POLONAISE'97—Seismic and gravimetric modelling of the crustal structure in the Polish Basin, *Phys. Chem. Earth*, *25*(4), 355–363, doi:10.1016/S1464-1895(00)00057-0.
Krzemiński, L. (2005), Provenance of Carboniferous sandstones from the Variscan foreland basins in southwestern Poland and Moravia (in Polish with English summary), *Biul. Państwowego Inst. Geol.*, *417*, 27–108.
Lenkey, L., P. Dövényi, F. Horváth, and S. A. P. L. Cloetingh (2002), Geothermics of the Pannonian basin and its bearing on the neotectonics, in *Neotectonics and Surface Processes: The Pannonian Basin and Alpine/Carpathian System*, *Stephan Mueller Spec. Publ. Ser.*, vol. 3, edited by S. A. P. L. Cloetingh et al., pp. 29–40, Copernicus, Katlenburg-Lindau, Germany.
Majdański, M., M. Grad, A. Guterch, and the SUDETES 2003 Working Group (2006), 2-D seismic tomographic and ray tracing modelling of the crustal structure across the Sudetes Mountains basing on SUDETES 2003 experiment data, *Tectonophysics*, *413*(3–4), 249–269, doi:10.1016/j.tecto.2005.10.042.
Majdański, M., E. Kozlovskaya, M. Grad, and SUDETES 2003 Working Group (2007), 3D structure of the Earth's crust beneath the northern part of the Bohemian Massif, *Tectonophysics*, *437*, 17–36, doi:10.1016/j.tecto.2007.02.015.
Majorowicz, J. (1976), Heat flow map of Poland on the background of geothermal field of Europe and some aspects of its interpretation, *Acta Geophys. Pol.*, *24*, 147–156.
Majorowicz, J. A., V. Cermak, J. Šafanda, P. Krzywiec, M. Wróblewska, A. Guterch, and M. Grad (2003), Heat flow models across the Trans-European suture zone in the area of the POLONAISE'97 seismic experiment, *Phys. Chem. Earth*, *28*, 375–391.
Málek, J., M. Brož, T. Fischer, J. Horálek, P. Hrubcová, J. Janský, O. Novotný, and R. Růžek (2001), Seismic measurements along short profiles in Western Bohemia during the CELEBRATION 2000 experiment, *Acta Montana IRSM AS CR, Ser. A*, *18*, 15–28.
Malinowski, M. (2005), Analysis of short-period Rayleigh waves recorded in the Bohemian Massif area during CELEBRATION 2000 experiment, *Stud. Geophys. Geod.*, *49*, 485–500, doi:10.1007/s11200-005-0023-3.
Malinowski, M., A. Żelaźniewicz, M. Grad, A. Guterch, T. Janik, and the CELEBRATION Working Group (2005), Seismic and geological structure of the crust in the transition from Baltica to Palaeozoic Europe in SE Poland–CELEBRATION 2000 experiment, profile CEL02, *Tectonophysics*, *401*, 55–77, doi:10.1016/j.tecto.2005.03.011.
Malinowski, M., M. Grad, A. Guterch, E. Takács, Z. Śliwiński, L. Antonowicz, E. Iwanowska, G. R. Keller, and E. Hegedűs (2007), Effective sub-Zechstein salt imaging using low-frequency seismics- results of the GRUNDY 2003 experiment across the Variscan front in the Polish Basin, *Tectonophysics*, *439*, 89–106, doi:10.1016/j.tecto.2007.03.006.
Malinowski, M., M. Grad, A. Guterch, and the CELEBRATION 2000 Working Group (2008), 3-D seismic modelling of the crustal structure between East European craton and the Carpathians in SE Poland based on CELEBRATION 2000 data, *Geophys. J. Int.*, *173*, 546–565, doi:10.1111/j.1365-246X.2008.03742.x.
Malkovský, M. (1979), Tectogenesis of the Bohemian Massif platform cover (in Czech), *Knihovna Ústředniho Ústavu Geol. Praha*, *53*, 1–176.
Matte, P., H. Maluski, P. Rajlich, and W. Franke (1990), Terrane boundaries in the Bohemian Massif: Result of large-scale Variscan shearing, *Tectonophysics*, *177*, 151–170, doi:10.1016/0040-1951(90)90279-H.
Mayerová, M., M. Novotný, and M. Fejfar (1994), Deep seismic sounding in Czechoslovakia, in *Crustal structure of the Bohemian Massif and West Carpathians*, edited by V. Bucha and V. Bližkovský, pp. 13–21, Academia Praha, Prague.
Mazur, S., and M. Jarosiński (2006), Deep basement structure of the Palaeozoic platform in SW Poland in the light of POLONAISE'97 seismic experiment (in Polish with English summary), *Prace Państwowego Inst. Geol.*, *188*, 203–222.
Mazur, S., P. Aleksandrowski, R. Kryza, and T. Oberc-Dziedzic (2006), The Variscan orogen in Poland, *Geol. Q.*, *50*(1), 89–118.
Mueller, H. J. (1995), Modelling of the lower crust by simulation of the in situ conditions: An example from Saxonian Erzgebirge, *Phys. Earth Planet. Inter.*, *92*, 3–15, doi:10.1016/0031-9201(95)03055-2.
Neunhöfer, H., and D. Güth (1989), Detailed investigation of the great earthquake swarm in Western Bohemia by the local Vogtland network, in *Monitoring and Analysis of the Earthquake Swarm 1985/86 in the Region Vogtland/Western Bohemia*, edited by P. Borman, *Veröffentlichungen Zentralinst. Phys. Erde*, *110*, 124–164.
Neunhöfer, H., and T. Meier (2004), Seismicity in the Vogtland/Western Bohemia earthquake region between 1962 and 1998, *Stud. Geophys. Geod.*, *48*, 539–562, doi:10.1023/B:SGEG.0000037471.18297.07.
Neunhöfer, H., F. Marillier, and G. F. Panza (1981), Crust and upper mantle structure in the Bohemian Massif from the dispersion of Rayleigh waves, *Gerlands Beitr. Geophys.*, *90*, 514–520.
Novotný, O., T. A. Proskuryakova, and A. V. Shilov (1995), Dispersion of Rayleigh waves along the Prague-Warsaw profile, *Stud. Geophys. Geod.*, *39*, 138–147, doi:10.1007/BF02296071.
Novotný, O., M. Grad, C.-E. Lund, and L. Urban (1997), Verification of the lithospheric structure along profile Uppsala—Prague using surface wave dispersion, *Stud. Geophys. Geod.*, *41*, 15–28, doi:10.1023/A:1023332522678.
Petecki, Z., O. Polechońska, E. Cieśla, and S. Wybraniec (2003), Magnetic map of Poland, scale 1:500,000, Pol. Geol. Inst., Warsaw.
Pharaoh, T. C. (1999), Palaeozoic terranes and their lithospheric boundaries within the Trans-European suture zone (TESZ): A review, *Tectonophysics*, *314*, 17–41, doi:10.1016/S0040-1951(99)00235-8.
Plomerová, J., U. Achauer, V. Babuška, and L. Vecsey (2007), Upper mantle beneath the Eger Rift (central Europe): Plume or asthenosphere upwelling?, *Geophys. J. Int.*, *169*(2), 675–682, doi:10.1111/j.1365-246X.2007.03361.x.
Pokorný, L., and L. Beneš (1997), Magnetic field, in *Geological Model of Western Bohemia Related to the KTB Borehole in Germany*, edited by S. Vrána and V. Štědrá, *J. Geol. Sci.*, *47*, 43–51.
Posgay, K., T. Fancsic, E. Hegedűs, Pápa, A. Bodoky, and E. Takács (2001), Metamorphic and geologic effects shown by seismic data in the Carpathian Basin, *Acta Geol. Hung.*, *44*, 113–134.
Prodehl, C., S. Mueller, and V. Haak (1995), The European Cenozoic rift system, in *Continental Rifts: Evolution, Structure, Tectonics*, *Dev. Geotect.*, vol. 25, edited by K. H. Olsen, pp. 133–212, Elsevier, New York.
Růžek, B., V. Vavryčuk, P. Hrubcová, J. Zedník, and the CELEBRATION Working Group (2003), Crustal anisotropy in the Bohemian Massif, Czech Republic: Observations based on Central European Lithospheric Experiment Based on Refraction (CELEBRATION) 2000, *J. Geophys. Res.*, *108*(B8), 2392, doi:10.1029/2002JB002242.
Růžek, B., P. Hrubcová, M. Novotný, A. Špičák, and O. Karousová (2007), Inversion of travel times obtained during active seismic refraction experiments CELEBRATION 2000, ALP 2002 and SUDETES 2003, *Stud. Geophys. Geod.*, *51*, 141–164, doi:10.1007/s11200-007-0007-6.
Šalanský, K. (1996), Magnetic map of the Czech Republic, in *Maps of the Czech Republic With a Resolution Corresponding to the 1:500 000 Scale* [CD-ROM], Czech Geol. Surv., Prague.
Špičák, A., J. Horálek, A. Boušková, Č. Tomek, and J. Vaněk (1999), Magma intrusions and earthquake swarm occurrence in the western part of the Bohemian Massif, *Stud. Geophys. Geod.*, *43*, 87–106, doi:10.1023/A:1023366210017.
Špičák, A., A. Förster, and B. Horsfield (2005), Drilling the Eger Rift in central Europe, *Sci. Drill.*, *1*, 44–46.
Środa, P. (1999), *Modifications of Software Package ZPLOT by C. Zelt*, Inst. Geophys. Pol. Acad. Sci., Warsaw.
Środa, P., and POLONAISE P3 Working Group (1999), P- and S-wave velocity model of the southwestern margin of the Precambrian East European craton; POLONAISE'97, profile P3, *Tectonophysics*, *314*, 175–192.
Środa, P., W. Czuba, M. Grad, A. Guterch, E. Gaczynski, and the POLONAISE Working Group (2002), Three-dimensional seismic modelling of crustal structure in the TESZ region based on POLONAISE'97 data, *Tectonophysics*, *360*, 169–185, doi:10.1016/S0040-1951(02)00351-7.
Środa, P., et al. (2006), Crustal and upper mantle structure of the Western Carpathians from CELEBRATION 2000 profiles CEL01 and CEL04: Seismic models and geological implications, *Geophys. J. Int.*, *167*, 737–760, doi:10.1111/j.1365-246X.2006.03104.x.
Švancara, J., I. Gnojek, F. Hubatka, and K. Dedacek (2000), Geophysical field pattern in the West Bohemian geodynamic active area, *Stud. Geophys. Geod.*, *44*, 307–326.
Szczepański, J. (2007), A vestige of Early Devonian active continental margin in the East Sudetes (SW Poland)—Evidence from geochemistry of the Jegłowa Beds, Strzelin Massif, *Geol. Q.*, *51*(3), 271–284.
Tait, J. A., M. Schätz, V. Bachtadse, and H. Soffel (2000), Palaeomagnetism and Palaeozoic palaeogeography of Gondwana and European terranes, in *Orogenic Processes: Quantification and Modelling in the Variscan Belt*, edited by W. Franke et al., *Geol. Soc. Spec. Publ.*, *179*, 21–34.
Tomek, Č., V. Dvořáková, and S. Vrána (1997), Geological interpretation of the 9HR and 503M seismic profiles in western Bohemia, *J. Geol. Sci.*, *47*, 43–50.

Vavryčuk, V., P. Hrubcová, M. Brož, J. Málek, and the ALP 2002 Working Group (2004), Azimuthal variation of Pg velocity in the Moldanubian, Czech Republic: Observations based on a multi-azimuthal common-shot experiment, *Tectonophysics*, *387*, 189–203, doi:10.1016/j.tecto.2004.06.015.

Vosteen, H.-D., V. Rath, C. Clauser, and B. Lammerer (2003), The thermal regime of the Eastern Alps from inversion analyses along the TRANSALP profile, *Phys. Chem. Earth*, *28*, 393–405.

Weiss, T., S. Siegesmund, W. Rabbel, T. Bohlen, and M. Pohl (1999), Seismic velocities and anisotropy of the lower continental crust: A review, *Pure Appl. Geophys.*, *156*, 97–122, doi:10.1007/s000240050291.

Wielandt, E., A. Sigg, A. Plešinger, and J. Horálek (1987), Deep structure of the Bohemian Massif from phase velocities of Rayleigh and Love waves, *Stud. Geophys. Geod.*, *31*, 1–7, doi:10.1007/BF01631100.

Wielandt, E., A. Sigg, A. Plešinger, and J. Horálek (1988), Deep structure of the Bohemian Massif from phase velocities of Rayleigh and Love waves, *Phys. Earth Planet. Inter.*, *51*, 155–156, doi:10.1016/0031-9201(88)90036-2.

Wilde-Piórko, M., J. Saul, and M. Grad (2005), Differences in the crustal and uppermost mantle structure of the Bohemian Massif from teleseismic receiver functions, *Stud. Geophys. Geod.*, *49*, 85–107, doi:10.1007/s11200-005-1627-3.

Winchester, J. A., and the PACE TMR Network Team (2002), Palaeozoic amalgamation of central Europe: New results from recent geological and geophysical investigations, *Tectonophysics*, *360*, 5–21, doi:10.1016/S0040-1951(02)00344-X.

Wybraniec, S. (1999), Transformations and visualization of potential field data, *Pol. Geol. Inst. Spec. Pap.*, *1*, 88 pp.

Żelaźniewicz, A., D. Marheine, and T. Oberc-Dziedzic (2003), A Late Tournaisian synmetamorphic folding and thrusting event in the eastern Variscan foreland: $^{40}Ar/^{39}Ar$ evidence from the phyllites of the Wolsztyn-Leszno High, western Poland, *Int. J. Earth Sci.*, *92*, 185–194.

Zelt, C. (1994), ZPLOT-An interactive plotting and picking program for seismic refraction data, report, Bullard Lab., Univ. of Cambridge, Cambridge, U.K.

Ziegler, P. A. (1990), *Geological Atlas of Western and Central Europe*, 2nd ed., 239 pp., Shell Geol. Soc. Publ. House, Bath, U.K.

Ziegler, P. A., and P. Dèzes (2005), Evolution of the lithosphere in the area of the Rhine Rift System, *Int. J. Earth Sci.*, *94*, 594–614, doi:10.1007/s00531-005-0474-3.

W. H. Geissler, Alfred Wegener Institute for Polar and Marine Research, Am Alten Hafen 26, D3210, D-27568 Bremerhaven, Germany.

M. Grad, Institute of Geophysics, University of Warsaw, Pasteura 7, 02-093 Warsaw, Poland. (mgrad@mimuw.edu.pl)

A. Guterch, Institute of Geophysics, Polish Academy of Sciences, Ks. Janusza 64, 01-452 Warsaw, Poland.

P. Hrubcová and A. Špičák, Geophysical Institute, Academy of Science of the Czech Republic, Boční II/1401, 141 31 Prague 4, Czech Republic.

G. R. Keller, School of Geology and Geophysics, University of Oklahoma, Norman, OK 73071, USA.

S. Mazur, GETECH, Kitson House, Elmete Hall, Elmete Lane, Leeds LS8 2LJ, UK.